NANOTRIBOLOGICAL PROPERTIES OF GRAPHENE GROWN ON SILICON CARBIDE SEMICONDUCTOR

A Thesis Submitted to
Graduate School of Engineering and Sciences of
İzmir Institute of Technology
in Partial Fulfillment of the Requirements for the Degree of

MASTER OF SCIENCE
in Materials Science and Engineering

by
Yasemin KESKİN

July, 2018
İZMİR

We approve the thesis of **Yasemin KESKİN**

Examining Committee Members:

Assoc. Prof. Dr. Cem ÇELEBİ
Department of Physics, İzmir Institute of Technology

Assist. Prof. Dr. Gökhan UTLU
Department of Physics, Ege University

Assoc. Prof. Dr. Müjdat BALANTEKİN
Department of Electrical and Electronics Engineering, İzmir Institute of Technology

9 July 2018

Assoc. Prof. Dr. Cem ÇELEBİ
Supervisor, Department of Physics,
İzmir Institute of Technology

Assist. Prof. Dr. Özhan ÜNVERDİ
Co-Supervisor, Department of
Electrical and Electronical Engineering,
Yasar University

Prof. Dr. Mustafa Muammer DEMİR
Head of the Department of Materials
Science and Engineering

Prof. Dr. Aysun SOFUOĞLU
Dean of the Graduate School of
Engineering and Sciences

ACKNOWLEDGEMENTS

It is my pleasure to acknowledge and express my gratitude those who helped me along the way to completion of this thesis.

Firstly, I would like to thank my parents for all of their patience and support through the whole process of my study. They did everything for my future and happiness.

I would like to thank my advisor Assoc. Prof. Dr. Cem Çelebi and co-advisor Assistant Prof. Dr. Özhan Ünverdi for all their help, patience and detailed reviewing all of my study. Without their support and guidance, I would never have been able to complete this study.

I wish to thank the other committee members of my thesis Assist. Prof. Dr. Gökhan Utlu and Assoc. Prof. Dr. Müjdat Balantekin for their participation and comments.

I would like to thank Hilal Gözler, Team Leader at NanoMagnetics Instruments with all my heart because she had never refused to explain the basics of AFM whenever I asked her. Also Arda Balkancı who helped me a lot, I would like to thank him for his knowledge and time.

I would like to acknowledge my lab mates and friends; Erdi Kuşdemir, Dilce Özkendir, Damla Yeşilpınar and Ece Meriç for their experimental knowledge and support during my study.

I wish to acknowledge using of facilities at the IKCU Material Research Center for SEM analysis. In addition, I would like to thank specialist of Material Research Center Evren Çulcular for his valuable friendship. I would also thank to Alper Yanılmaz for Raman measurements and Mehmet Fidan for Epitaxial growth of samples.

I also would like to thank Mehmet Kürşat Uçur, Çağla Sarvan and Erinç Cibil for their valuable friendship and support.

I would also thank to Cem Erdoğan and his sweet family who believe me and stand by me in every condition.

ABSTRACT

NANOTRIBOLOGICAL PROPERTIES OF GRAPHENE GROWN ON SILICON CARBIDE SEMICONDUCTOR

In this thesis, nanotribological properties of single and multilayer graphene grown on two sides of the Silicon Carbide (SiC) semiconductors were investigated. For this purpose, epitaxial growth technique was used to obtain single-layer graphene on both C-face and Si-face. This thesis consists of two purposes: One of them is to investigate the nanotribological properties of the single and multilayer graphene grown on C-face of SiC and the other one is to compare nanotribological properties of the single layer graphene on two sides of SiC. Graphene, a two-dimensional semi-metal material, was grown epitaxially on the SiC surface under ultra-high vacuum conditions. In epitaxial method, direct current heating is applied to the SiC substrate to vaporize Si atoms from the surface. As the Si atoms evaporate, the remaining C atoms form a graphene layers on top. When single layer graphene is formed on the Si-face, multilayer graphene is formed on the C-face at the same parameters. For this reason, two different samples of graphene were needed in order to compare the tribological properties of the single layer graphene grown on both Si-face and C-face for the secondary objective. A capping method was used to control the rate of Si atoms evaporating from the SiC surface. By this way, single layer graphene on the C-face was obtained too. Number of layers were determined by Raman Spectroscopy. Nanotribological characterizations were done with Atomic Force Microscopy. The experimental results showed that single layer graphene on the Si-face has higher friction coefficient compared to single layer graphene on the C-face. It has been found that the single layer graphene (0.02) formed on the C-surface has a lower coefficient of friction than the multilayer graphene (0.82). It is expected that with the support of the theoretical studies on this results will increase the interest in this study by means of these results are new and original for the literature.

ÖZET

YARIİLETKEN SİLİSYUM KARBÜR ÜZERİNDE BÜYÜTÜLEN EPİTAKSİYEL GRAFENİN NANOTRİBOLOJİK ÖZELLİKLERİ

Bu tezde, Silisyum Karbür (SiC) yarı iletkeninin iki yüzü üzerinde büyütülen tek ve çok katman grafenin nanotribololojik özellikleri incelendi. Bu amaçla, hem karbon (C-) hem de silikon (Si-) yüzeyi üzerinde tek katman grafen elde etmek için epitaksiyal büyüme tekniği kullanıldı. Bu tez, iki temel amaç olan C- yüzeyi üzerinde oluşan tek ve çok katman grafenin nanotribolojik özelliklerini inceleme ve iki yüzey (Si-yüzü ve C-yüzü) üzerinde oluşan tek katman grafenin sürtünme özelliklerini kıyaslamaya yönelik çalışmaları içermektedir. 2 boyutlu yarıiletken bir malzeme olan grafen, ultra yüksek vakum altında SiC yüzeyi üzerinde epitaksiyel yolla büyütülmüştür. Belirli parametrelerde SiC alttaşı yüzeyine doğrudan akım uygulayarak yüzey üzerinden Si atomlarının buharlaştırılması sağlanmaktadır. Si atomları buharlaşırken geriye kalan C atomları grafeni oluşturmaktadır. Si- yüzeyi üzerinde tek katman grafen oluşurken, aynı parametrelerde C- yüzeyinde çok katmanlı grafen oluşur. Bu nedenle ikincil amaç olan Si- yüzü ve C- yüzündeki tek katman grafenin tribolojik özelliklerini kıyaslayabilmek için iki ayrı grafen örneğine ihtiyaç duyulmuştur. SiC yüzeyinden buharlaşan Si atomlarının hızını kontrol altına almak için kapaklama (*capping*) yöntemi kullanıldı. Bu sayede C-yüzeyi üzerinde de istenilen tek katman grafen elde edilmiştir. Katman sayısının tayini Raman Spektroskopisi ile gerçekleştirildi. Nanotribolojik karakterizasyon Atomik Kuvvet Mikroskobu ile yapıldı. Elde edilen deneysel sonuçlar, Si-yüzündeki tek katman grafenin, C-yüzündeki tek katman grafenden yüksek olduğunu göstermektedir.Ayrıca C-yüzeyinde oluşan tek katman grafenin (0.02) çok katman grafene (0.82) kıyasla daha az sürtünme katsayısına sahip olduğu saptanmıştır. Bulunan bu sonuç literatürde özgün ve yeni olmakla beraber teorik verilerle desteklendiğinde bu çalışmaya yönelik ilgiyi artıracağı beklenmektedir.

To my family,

TABLE OF CONTENTS

LIST OF FIGURES

Figure **Page**

LIST OF TABLES

LIST OF ABBREVIATIONS

SiC……...Silicon Carbide

SEM……Scanning Electron Microscopy

AFM……..…Atomic Force Microscopy

2D…….……Two-dimensional

UHV…….Ultra-High Vacuum

FFM……..…….Friction Force Measurements

EG……...Epitaxial graphene

SiO_x……...…..Silicon Oxide

CHAPTER 1

INTRODUCTION

1.1. Tribology

Tribology means the science and technology of two interacting surfaces in relative motion and of related subjects and practices.[1] The known studies of tribology are friction, wear, and lubrication. As the new techniques emerge by measuring surface topography, adhesion wear and friction and also lubricant material's thickness has led to developments of new fields which are called Nanotribology, Microtribology and Atomic-Scale Tribology etc.

Tribology is concerned with theoretical and experimental studies of processes ranging from atomic and molecular scales to microscale happen adhesion, friction, wear, and thin-film lubrication at sliding surfaces. These studies are needed to develop a basic understanding of interfacial phenomena at a small scale and to examine interfacial phenomena in micro- and nano-structures used in magnetic storage systems, microelectromechanical systems (MEMs) and other industrial applications[1]. As the development of tribology on nanoscale, many physicists and chemists have contributed to fundamentals of friction and wear. Consequently, tribology is now worked by both engineers and scientists. It is growing rapidly and it has become very popular as tribologists study this new field of micro and nanotribology since 1991[1].

The name tribology comes from the Greek name "*trib*o", that means "to rub, therefore Jost gave its literal translation "the science of rubbing" in 1966 [2].

The tribology explains the introduction of sliding at the interface and study of friction in the presence of lubricant materials. There are a lot of scientist who has been studied the friction. It was first explored by the Egyptian ancestors in BC by trying to push the large monuments one place to another by using water as liquid lubricant material and Figure 1 represents the approximately 170 slaves while transporting the Colossus.

Dowson, 1979, has estimated that each man exerted a pull of about 800 N. The total effort, which must at least equal the friction force, becomes 172 x 800 N. Thus, the coefficient of friction is about 0.23 [1].

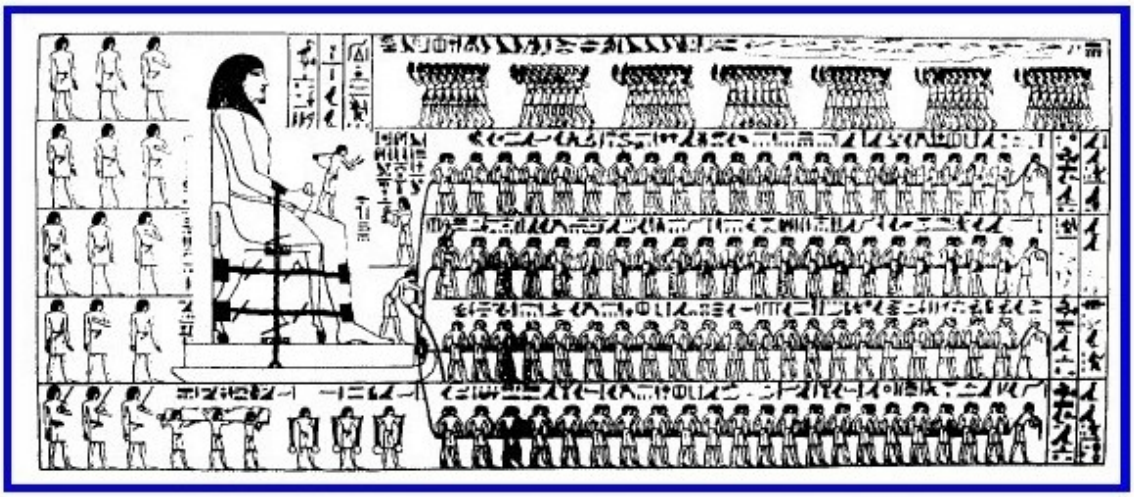

Figure 1. Egyptians using lubricant to aid movement of Colossus, El-Bersheh, circa 1800 BC[1]

Dowson, 1979, has estimated that each man exerted a pull of about 800 N. The total effort, which must at least equal the friction force, becomes 172 x 800 N. Thus, the coefficient of friction is about 0.23 [1].

But before this estimation, first concept of friction was studied by Leonardo Da Vinci which tells us that friction force is directly proportional to the normal load as seen in Equation 1.1 . In addition to this study, in 1966 the most important postulation were declared by Amontons that friction force is independent of the apparent area of contact as seen and Figure 2 . In 1781 these observations were confirmed by Coulomb, who established a clear distinction between static and kinetic friction.

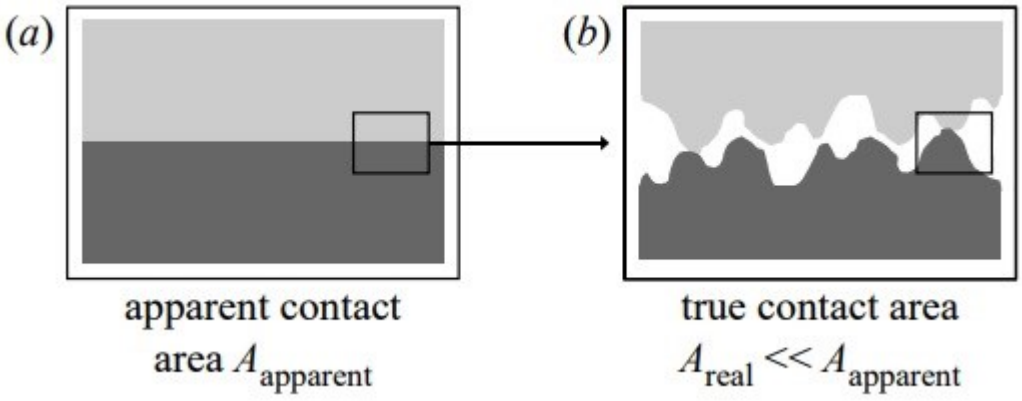

Figure 2. Schematics illustrating the basic concept of nanotribology[3]

In micro and nano structures, components are very light and operate under very light loads so, the friction and wear of lightly loaded nano components are heavily dependent on surface interaction in nanoscale and microscale and also single asperities plays very important role at nanoscale as seen in Figure 2[3]. Micro and nano tribological techniques are ideal for studying the friction and wear processes of micro and nano structures. These researches are also valuable in the fundamental understanding of interfacial phenomena in macrostructures to get a connection between science and engineering. Friction have been found smaller compared to macroscale so micro-nanotribological studies can explain the ultra-low regime of friction and zero wear.

Amontons' Law of Friction;

$$F_f = \mu F_{load} \tag{1.1}$$

It is working in the case of Coulomb friction without lubrication. The frictional force between two interacting bodies is typically described by the law of friction where the F_{load} represents the external loading force and μ is the friction coefficient. This situation is valid when sliding occurs without lubrication. But understanding of three fundamental mechanism of friction on the atomic scale is relatively limited since the most macroscopic and microscopic frictional effects are dominated by the influence of wear, plastic deformation, lubrication, surface roughness and surface asperities. So the macroscopic friction experiments are difficult to analyze in terms of universal theory[3]. In the last few decades nanotribology comes out by introducing new experimental tools such as AFM.

1.2. Graphene

Graphene is a 2D and zero band gap semi-metal which consists of hexagonally closed packed carbon atoms. Graphene has no band gap. The conduction and valance band intersect within the Dirac cone at which all fermi electrons act like massless particle as can be seen in Figure 3 .

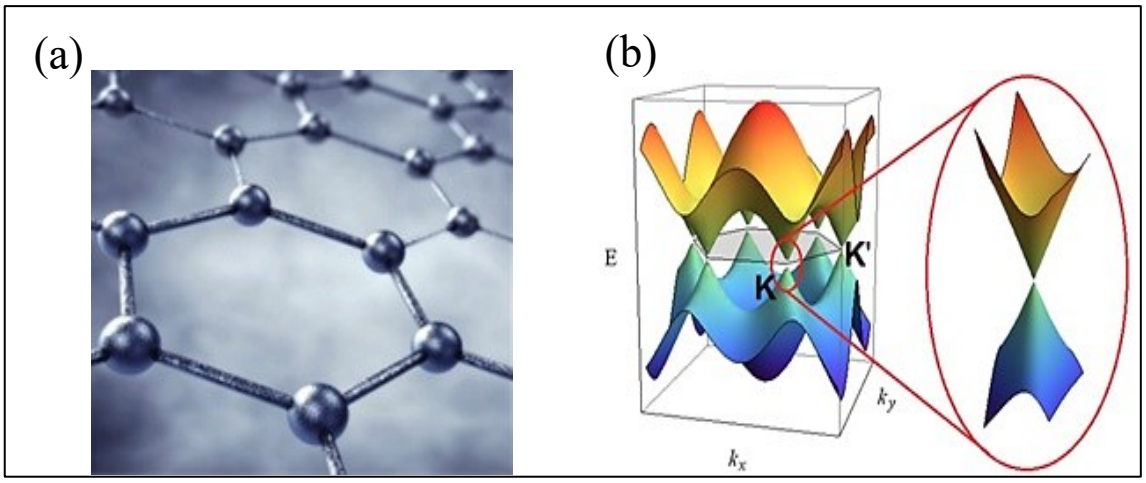

Figure 3. (a) Atomic structure of single layer graphene (b) Energy dispersion of single layer graphene

It can be produced by several methods. In 2010, A. Geim and K. Novoselov won the Nobel Prize as they succeeded in producing graphene flakes by mechanically exfoliation technique 4. By the help of this method, graphene flakes with low defect concentration and high mobility can be obtained at nano-scale. There is another method for obtaining graphene which is called epitaxial growth technique.

While mechanical exfoliation method is very simple to obtain micro-scaled graphene, in contrast, uniform and homogeneous graphene flakes can be obtained by epitaxial growth method. On the other hand, no matter how large the graphene flakes can be obtained by CVD method, there are lots of harmful chemicals to produce single layer CVD graphene. Also after the CVD growth, the graphene has to be transferred to SiOx for using in several applications such as transistors.

1.3. Graphene and Its Properties

As the considerable requirement of micro and nanoscale devices is on the rise, solid materials that reduce friction has begun to be investigated for tribology studies at micro/nano scale. One of the most suitable material as a solid lubricant is graphene which has unique properties such as extraordinary mechanical strength beyond its electronic, optical and chemical properties. Reducing friction and showing unexpected properties arouse attention to the investigation of graphene's tribological behavior.

The motivation of this study was the comparison of multilayer and single layer graphene grown on C-face SiC. Some difficulties in the synthesis of graphene grown on C-face SiC did not allow any tribological work to be done on this area. At the beginning of these difficulties, it is not easy to control the number of graphene layers formed on the C surface while compared with the Si-face. Since the synthesizing graphene on C-face under UHV conditions is a fact and theoretical studies are still wondered, it was aimed to observe the frictional properties of graphene layers grown on C-face SiC. Due to the discrepancy in electronic, structural and sliding properties of graphene grown on Si and C faces, different frictional characteristics are expected.

Several studies of the tribological characteristics of epitaxially grown graphene were performed with only graphene grown on Si-face side of SiC semiconductor and also it was compared with other synthesizing techniques such as exfoliated and CVD graphene. Erdemir et.al showed that graphene can reduce the rate of wear and the coefficient of friction of steel. Evidently reduction in friction and wear refers that low shear and highly protective behaviour of graphene do not allow steel surface to be oxidized while sliding the contact surfaces[5].

Depending on AFM studies, there are large number of studies that examine the nanotribological properties of the graphene. One of them was M. Baykara and his co-workers' study. In this study, 5 PPPCONTR Silicon tips were calibrated on the trapezoidal shape of TGF111 test grating samples by using Sader and Varenberg studies respectively [6,7] and the force distance calibration were done in order to find the desired force acting on the test grating. CVD graphene transferred onto the SiO_x substrate and normal spring constants and calibration constants were calculated. In this study, 5 different tips were calibrated and the friction coefficient on the SiO_x surface of the graphite is reduced by 90 %. Also it has been observed that it exhibits an effective solid lubricant material property.

Also the tribological comparison of single layer graphene grown on Si-face and C-face has been studied in this thesis. There are lots of studies about frictional properties of graphene that synthesized by some other methods such as mechanical exfoliation and chemical vapor deposition (CVD) compared to the epitaxial graphene.

CHAPTER 2

EPITAXIAL GRAPHENE

2.1. Structure of SiC and Epitaxial Graphene

Silicon carbide is an important structural ceramic material which has higher heat resistance than Si. It has excellent oxidation resistance, strength containment to high temperatures (~ 2829 °C), high wear resistance, high thermal conductivity, and good thermal shock resistance due to its highly covalent (up to 88 %) chemical bonding between silicon and carbon atoms (distance between C and Si ~1.86 Å) [8,9]. It exhibits a wider band gap that has gained substantial attention for many applications such as MEMs and power electronics.

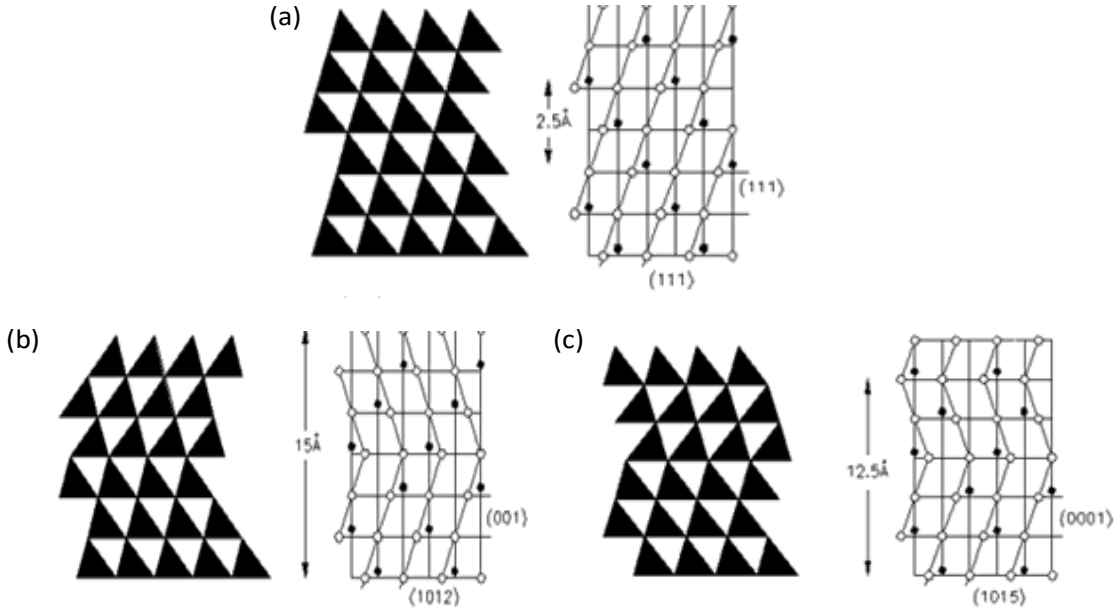

Figure 4. Representation of stacking sequence of (a) 3C-SiC, (b) 6H-SiC, (c) 4H-SiC[8]

Table 1. Properties of commonly used polytypes of SiC[10]

	Polytype	Stacking Sequence	Band Gap (eV)	Lattice Constants (Å)
(a)	3C	ABC	2.390	4.3596
(b)	6H	ABAC	3.023	3.0730
(c)	4H	ACB	3.263	3.0730

The bond length of Si and C is 1.89 Å and length between two layers is 2.52 Å [11]. SiC has two face sides which are SiC (0001) surface that face by Si atoms and SiC (000-1) surface that face by C atoms shown in Table 1[10]. These two face sides alter different properties after growth mechanism of graphene.

Silicon carbide has several types which is called polytype as can be seen in Figure 4 with respect to its stacking sequence [8]. In spite of the fact that countless polytypes are known and all around reported, not many of them are thought to be thermodynamically steady. Nonetheless, by all accounts, to be five little period polytypes (2H, 3C, 4H, and 6H) which are considered as fundamental SiC structures and which are found to happen generally as often as possible [12]. Table 1 represents an example of the stacking sequence of (a) 3C-SiC (b) 6H-SiC, (c) 4H-SiC [13].

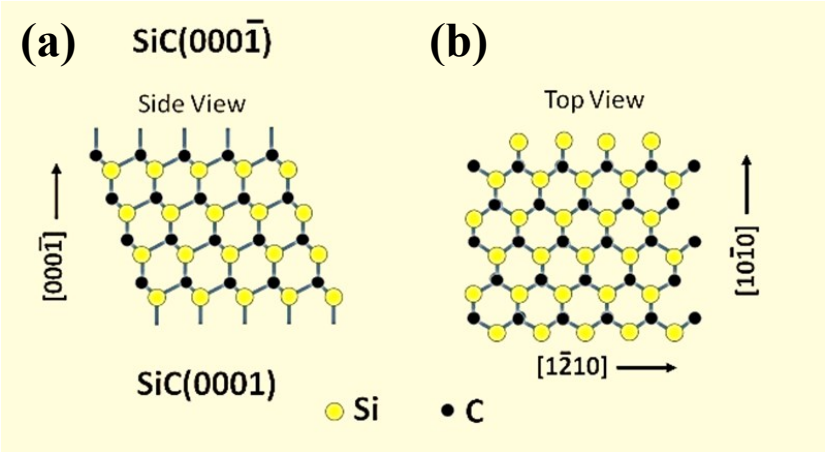

Figure 5. (a) Side view and (b) top view of 6H-SiC[13]

In this study, for the comparison between single layer graphene grown on the Si-face and the C-face under UHV conditions, capping method was done in order to obtain single layer graphene on the C-face. Two samples were prepared to compare their

frictional properties. These are epi-ready C-face and epi-ready Si face which are exposed to only conventional cleaning procedure for removing organic compounds and native oxide from the surface, graphene grown on epi-ready C-face, and graphene grown on Si face. For epitaxial growth, direct current heating was applied on the samples to evaporate Si atoms from the surface. During the application of current through the samples, the temperature increases step by step up to ~1500 °C.

Graphene is grown much slower on the Si-face compared to the C-face 14. According to the literature, electron mobility of graphene which is grown on Si-face and under UHV conditions changes between 24 - 530 $cm^2V^{-1}s^{-1}$. Also it was mentioned that charge carrier density of graphene grown the Si-face is about 0.03 -5.10 x 10^{13} cm^{-2} [15].

Graphene grown on the C-face and the Si-face under UHV conditions has different properties. While reconstruction of Si-face is $(6\sqrt{3}$ x $6\sqrt{3})$ R30°, and it rotates well-ordered graphene formed on the SiC leaded to the interface layer between single and few layer graphene[16]. On the other hand, reconstruction of graphene on C-face is 2 × 2 and 3 × 3[17]. Because of the turbostatic force between graphene layers on C-face SiC, there is a rotation by 30° which effects the graphene to grow individually[18].

By the enlightenment of these extraordinary properties of epitaxial graphene grown on different side of SiC, it was aimed to obtain different results that helps to improve the literature.

2.2. Nanotribology of Epitaxial Graphene

Tribology is one of the most interesting topics in today's research. As mentioned before, one of the most effective ways to control friction is to use a lubricant in liquid and/or solid forms. One of the most suitable material is a two-dimensional and semi-metallic graphite with a single atomic thickness which is called graphene.

It is very crucial to understand the mechanical behavior and internal friction mechanism of graphene for efficient usage. Graphene, which can be obtained by several methods, is regarded as a suitable candidate as a solid lubricant [19]. Besides its electronic, mechanical and optical properties which are the focus of interest in epitaxial growth under ultrahigh vacuum, the ability of the graphite to be atomically fine-grained and conformal, graphene increase friction micro-scale and nano-scale and it can be used in MEMs / NEMs devices that have resistance to prolong the wear life[20].

Epitaxial growth of graphene on SiC semiconductor under UHV conditions for tribological study is very intriguing. Comparing the graphene grown on C face and Si face, J. Hass et.al claimed removing all Si atoms from the bilayer surface leaves a C-face surface to which the nucleating graphene apparently does not bind covalently so the graphene nuclei experience weak constraints [21] . Due to the discrepancy in electronic, structural and sliding properties of graphene grown on Si and C faces, different frictional characteristics are expected.

In the work of T. Filleter and his group, the friction of single and two layer graphene obtained epitaxially on SiC substrate. In this study, single layer graphene was grown epitaxially on 6H (0001) and friction and wear measurements were done. Also, single layer, bi-layer and multilayer graphite were compared and it was found that single layer graphene is more lubricant compared to graphite. Single layer graphene revealed that it is two times lubricant compared to the bi-layer graphene. The reason of this explained by electron-phonon coupling after taking ARPES (Angle-Resolved Photoemission Spectroscopy) measurements. Although the load dependence of friction for graphite and bilayer are the same, graphite has higher friction due to a load-independent offset which indicates a stronger adhesion[22]. Increase in adhesion was attributed to a larger contact area of the more compliant bulk graphite. graphite due to low adhesion[22,23]. Also the best lineer fit of friction force due to normal load had been occurred even at zero load. The reason was mainly attributed to the capillary force, electrostatic force, adhesion and Van der Waals force[23,24].

Friction force measurements were taken under ultrahigh vacuum assisted by AFM. The surface structure and the number of layers were determined by Raman Measurements. Multi and single layer graphene layers were detected by taking lots of data from the surface. When compared the results, it was observed that bi-layer, single layer and the graphite have the similar linearity behavior. In addition to this, graphite exhibits a strong adhesion property even though its strength is higher than graphene[25].

CHAPTER 3

SAMPLE PREPARATION

3.1. Sample Cleaning

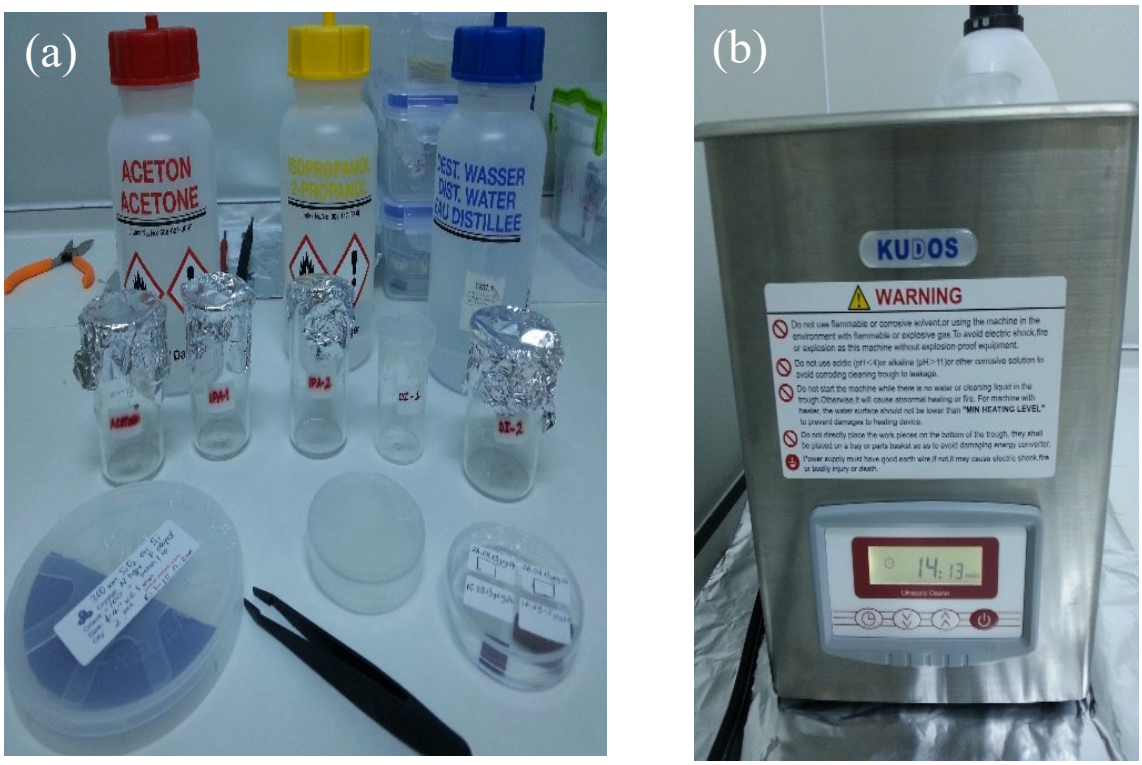

Figure 6. (a) Chemicals used for cleaning the substrates and (b) ultrasonic bath for the cleaning

We used two SiC substrate in order to conduct the friction force measurements. Before these experiments, SiC substrates need to be cleaned before the epitaxial experiments. Epi-ready Si-face and C-face SiC samples were diced into 4 x 10 mm^2 rectangular substrates. First of all, certain laboratory cleaning procedure was done to remove the organic contaminations (acetone, alcohol and IPA, Sigma Aldrich, ≥ 99 %). For this purpose each substrates were exposed to ultrasonic bath 15 minutes as can be seen in the Figure 6 . By this method organic contaminations will be removed easily.

After this process, the samples were exposed to diluted HF (6 %) solution. This process is very important to remove the native oxide on the SiC substrate.

3.2. Growth of Epitaxial Graphene on SiC Substrate

Graphene is one of the allotrope of carbon, one layer structure of C atoms arranged in a honeycomb lattice whose C - C length is about 0.142 nm. Epitaxial growth is very suitable for producing graphene since SiC hexagonal structure has perfect match with the graphene lattice. The most controllable process for graphitization of SiC surface is epitaxial growth technique which has known since 1975[26].

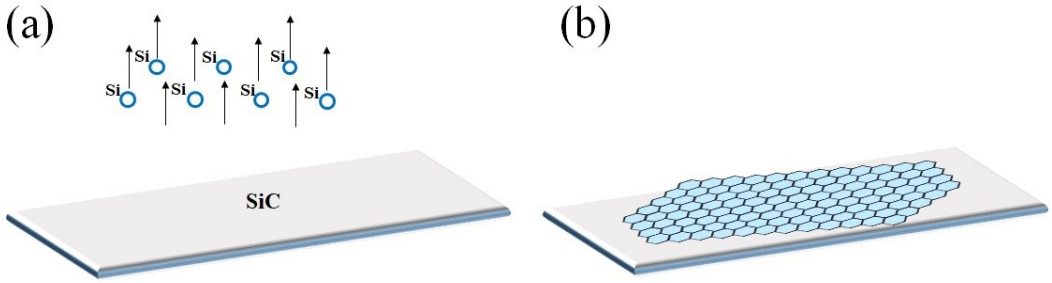

Figure 7. Schematic of epitaxial growth mechanism on SiC substrate (a) Sublimation of Si atoms in UHV and (b) remaining C atoms form graphene on SiC

Basically, Si atoms evaporate from the SiC substrates at very high temperature above 1300 °C. As these elevated temperatures, Si atoms evaporate from SiC substrate, then the remaining C atoms form graphene with the dangling bond which is created by the Si atoms as seen in Figure 7 . Next graphene layer forms as the same which is bonded with van der Waals forces. The reconstruction of C atoms on top of SiC is different for Si-face and C-face [27].

For the epitaxial growth experiments, ultrahigh vacuum (UHV) chamber were used where the base pressure was about 10^{-10} mbar. By this method, direct current heating method were applied through the sample. An optical pyrometer was used to measure the temperature of the sample with a resolution of ± 1 °C. For the growth steps, two different pumps were used. One of them is the turbo molecular pump and the other one is scroll pump. Scroll pump decreases the system pressure under 10^{-2} mbar to clean contamination inside the vacuum chamber. For the epitaxial growth of graphene on SiC substrate, the optimum growth pressure is at the range of 10^{-10} mbar. Two vacuum gauges were used to set the pressure of the system which are AUX1 (Cold Cathode) and IMG (Inverse

Magnetron Gauge). The pressure is measured by IMG between 10^{-3} mbar and 10^{-9} mbar as shown in Figure 8 .

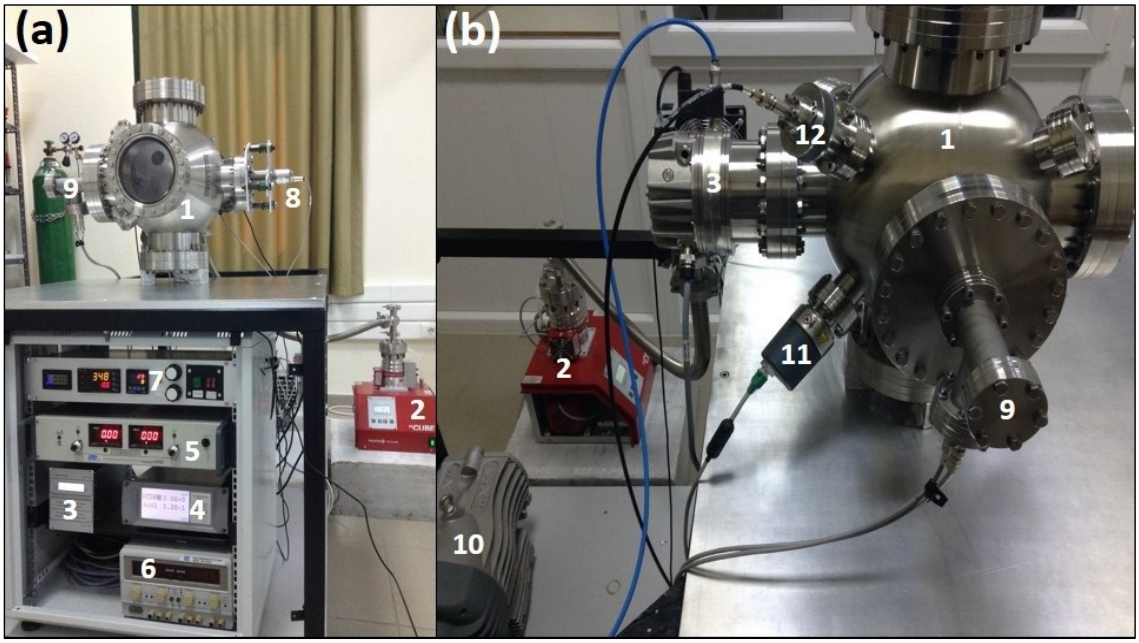

Figure 8. (a) (b) Vacuum System and Control Panel 1- Vacuum Chamber 2- Combined Pump 3- Turbo molecular pump and control panel 4- Gauge and Controller 5- DC power supply (Lambda Countant) 6- DC power supply (GW Instek) 7- Annealing system 8- Pyrometer 9 Annealing Set up of SiC 10- Scroll Pump 11- Gauge (Varian FRG-700) 12- Gauge (Varian IMG-300).

In order to get rid of organic contamination, the sample was annealed at 600 ℃ overnight. To remove the native oxide layer from the sample surface, the sample was heated up to 1050 ℃ for 5 min. In this way, the grain boundaries of the SiC substrate become larger at temperature 1300 ℃ within 7 min. Si atoms start to evaporate from the surface at 1350 ℃ and remaining carbon atoms form the graphene structure on SiC surface. The growth temperature and time are proportional to each other while obtaining monolayer (1350 ℃, 3 min.), few layer (1400 - 1450 ℃, 5 - 10 min.) and multilayer (1500 ℃, 20 min) graphene layers from the Si-face of SiC. For the graphene on C- face, there are more few steps to add these procedure. This capping method is used to increase the silicon vapor pressure during the annealing process to control the number of graphene layers on the C- face during the epitaxial growth.

The growth experiment for graphene grown on SiC was done in three steps. Before growth, SiC substrates were degassed at 600 ℃ overnight. This step is necessary for cleaning the organics from the sample surface. In order to remove oxide layer from the

sample surface, substrates were heated up to about 1050℃ for 5 min. After that in order to enlarge the grain boundaries of the SiC substrate, the temperature was increased to 1300 ℃ for 7 min. These procedures were same for each sample before the growth step. Above 1350℃, Si atoms begin to evaporate from the sample surface and remaining carbon atoms form graphene structure on the SiC surface. The optimum parameters for obtaining single and multilayer graphene on both C-face and Si-face were shown in the Table 2.

Table 2. Growth parameters for graphene on both sides

	Thermal Cleaning	**Oxide Removal**	**Surface Prep.**	**Growth**	**Cooling down**
Degree (°C)	600	1050	1300	1450	600
Time (min)	180	10	7	6	60

3.2.1. Growth of Graphene on Si-face of SiC

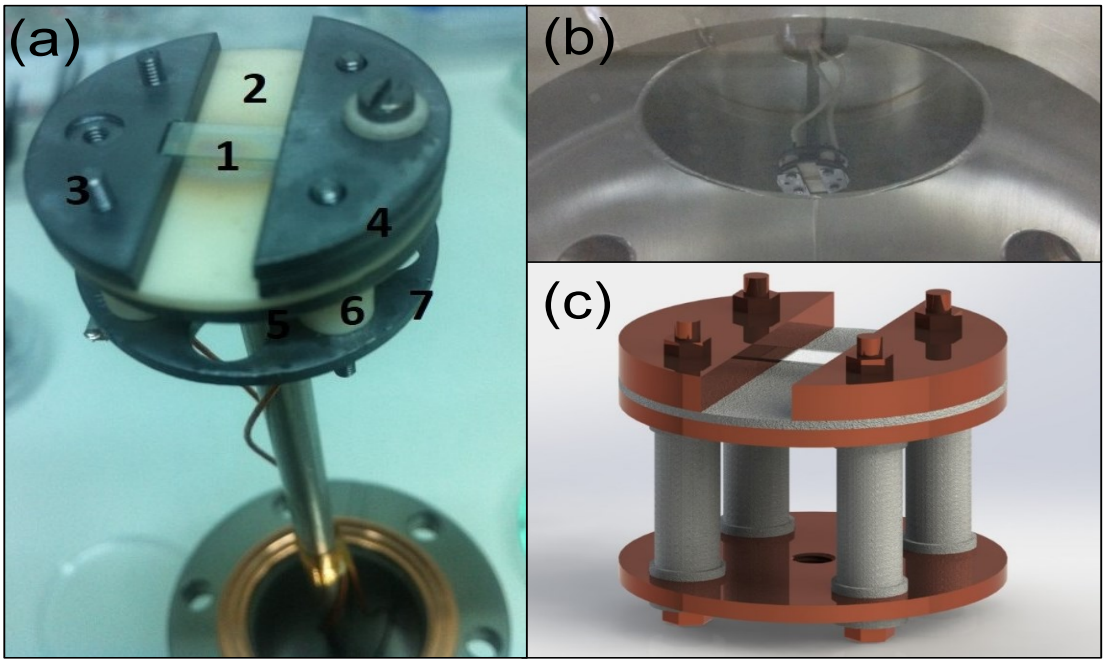

Figure 9. (a) SiC annealing set 1- SiC substrate 2- Alumina ceramic plate 3- tantalum screw and nuts 4- Tantalum or Molibdenium plates 5- Tantalum plate 6- Alumina ceramic beads 7- tantalum plate. (b) View of the sample holder with sample inside the vacuum chamber (c) Image of the sample obtained from 3D Modeling Program.

By the epitaxial growth method, graphene can be grown on both sides of SiC but thickness difference of graphene layers occurs because the formation rate of graphene on the C-face is higher than on Si-face. In order to obtain one-layer graphene on the C-face, the capping method was employed because it is possible to control the high sublimation rate of Si atoms with this method.

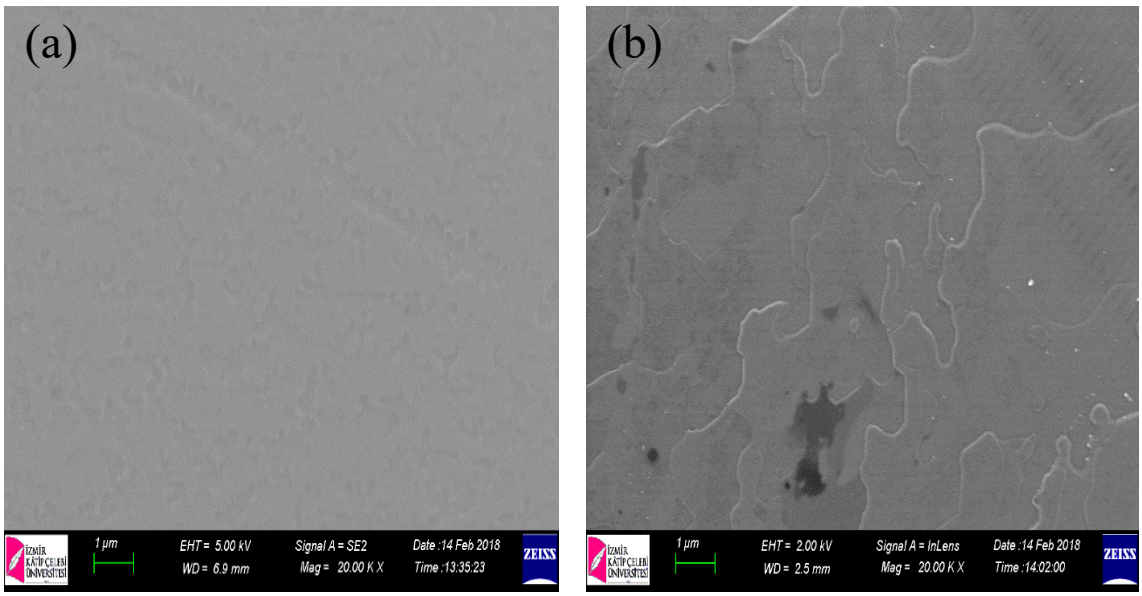

Figure 10. (a) SEM images of graphene grown on the Si-face of SiC and (b) on the C-face of SiC

In Figure 10 (a) and (b) shows the graphene grown on the Si-face and C-face of SiC substrate respectively.

3.2.2. Growth of Graphene on C-face of SiC

As mentioned before, Epitaxial graphene forms at temperatures above 1300°C both on the Si-face (0001) and C-face (000^{-}1) of a SiC semiconductor under UHV conditions. Unlike on the Si-face, graphene layers grown on the C-face surface of SiC are rotated with respect to the underlying substrate and the adjacent graphene layers are electronically decoupled from each other which is caused by their rotational stacking disorientation [28]. Each layer on the C face of SiC behaves like individual free-standing graphene which is very interesting for fundamental and technological research because of their unique stacking structure[29]. The carrier mobility of graphene layers on the C-face

of SiC has been measured to be approximately 10^5 cm^2 $V^{-1}s^{-1}$ which is much higher than the mobility of a single layer graphene grown on the Si-face surface of SiC [30,27].

The growth of high quality graphene with full coverage on the C-face surface of SiC is somewhat difficult. For example, extremely high sublimation rate of Si during the vacuum annealing process leads to the formation of high concentration crystalline defects in the graphene matrix and this makes difficult to control the number of layers with desired precision on that particular polar surface [26,31,18].

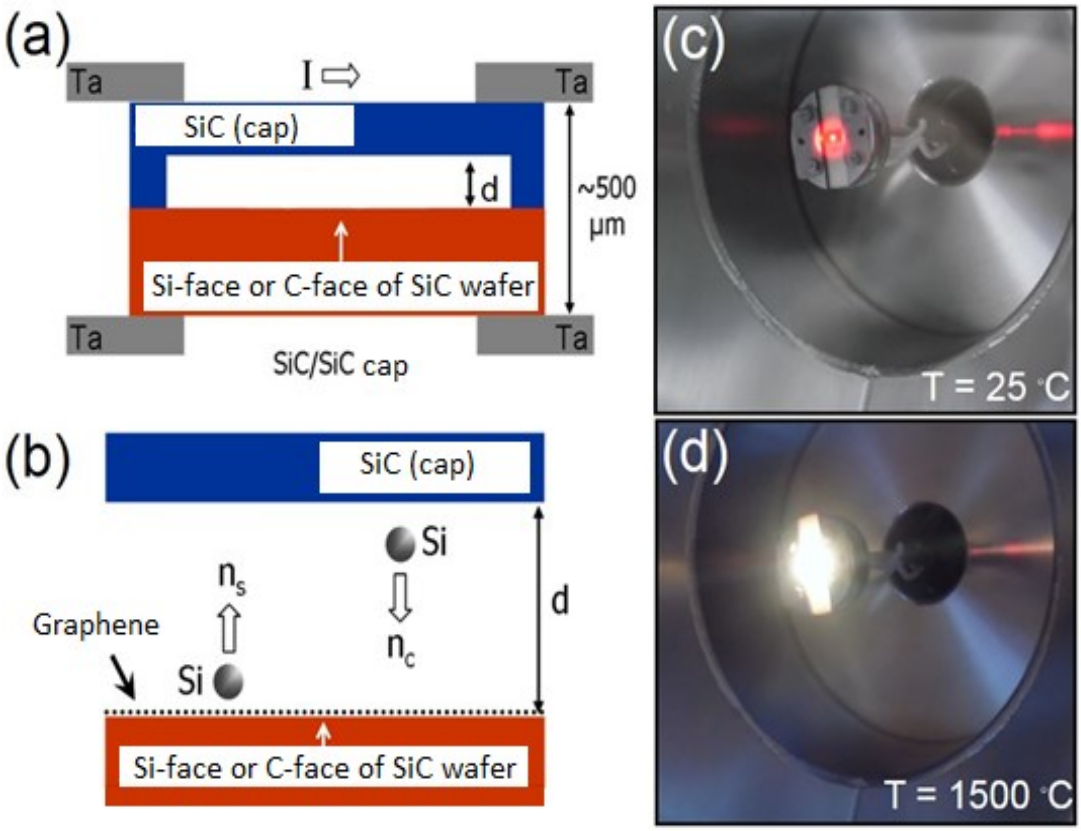

Figure 11. (a) Capping method of SiC (b) Sublimation of Si atoms from the Si-face or C-face of SiC wafer (c) Controlling of sample temperature with optical pyrometer (d) The growth temperature reaches 1500 ºC by direct current heating

Capping method was demonstrated in Figure 11 .Since direct current heating was applied on SiC substrate, Si atoms evaporate from SiC surface while C atoms formed graphene on the C-face SiC substrate. In capping method, two SiC substrate were put on top of each other. This will create a cavity between these substrates. The cavity between these two substrates will reduce the sublimation rate of Si atoms from the SiC substrate.

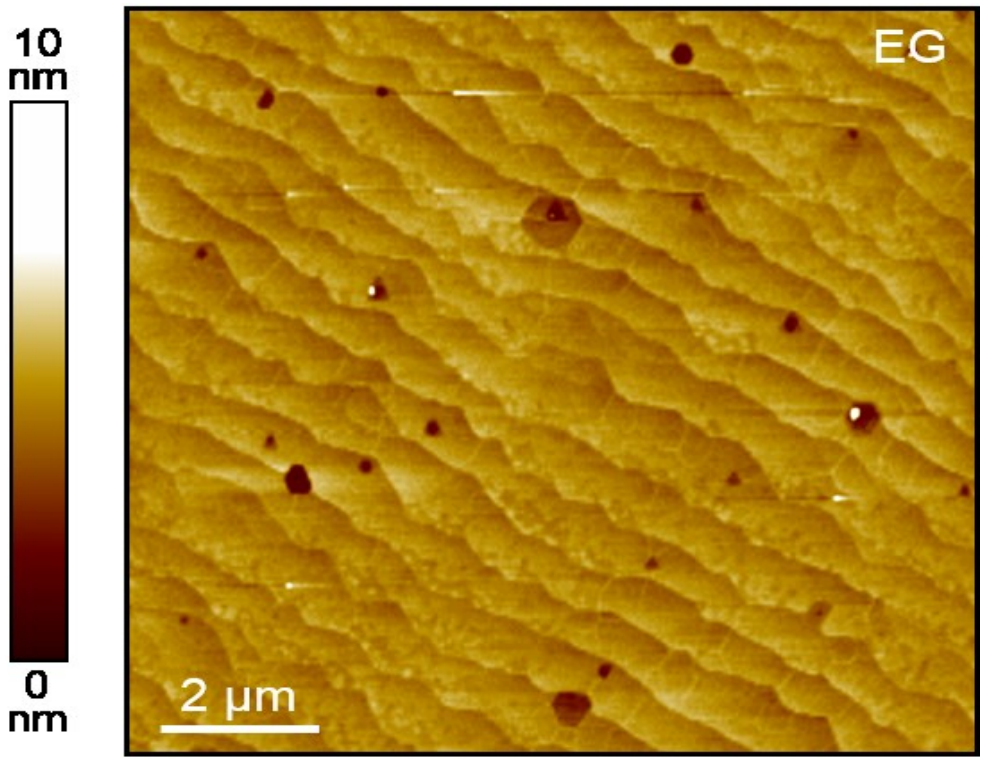

Figure 12. AFM topography image of graphene grown on the C-face of SiC

After chemical cleaning of the wafers diced into 4 mm wide and 10 mm long rectangular substrates, the sample was degassed overnight at around 600ºC and the remaining surface oxide layer was removed thermally by annealing the sample for about 8 min at around 1050 - 1100 ºC before the growth experiment.

As the capping substrate, a SiC crystal with the same dimensions was used, however with d = 300 nm deep, 3 x 3 mm^2 cavity etched on its Si-face surface. Prior to covering the C-face surface of SiC substrate, the capping substrate was annealed individually in UHV for about 15 min at 1430 ºC. This step is necessary for removing any trace of surface oxide and possible contamination and also it passivates the surface layer on the capping substrate. When the both substrates are attached on top of each other, the cavity on the capping substrate provides a well defined separation between them [29].

This new alternative method which is called the capping method and is very suitable for controlling the amount of the layer formed on the C-face. Celebi et.al showed that the capping of C-face SiC with another SiC significantly decreases the high growth rate of epitaxial graphene on the C-face surface even under UHV conditions. Uniform and thin layers can be produced with this method by locally confining the sublimated Si atoms in a half open cavity at the interface between a stack of two SiC substrates [29].

Graphene forms much slower on the Si-face when compared to C-face [32,14]. While increasing annealing temperature and time, it is possible to obtain the surface structure as more equilibrium state[15].

As shown in Figure 12 , the morphology of the single layer graphene can be determined by tapping mode AFM topography measurements. The AFM image of epitaxial graphene shows typical SiC background based large terraces In addition, graphene related flaky structures with blurry wrinkles lying on these terraces can be seen as well. The small amount of local but darker regions corresponds to a few layer graphene flakes [33].

3.3. Characterization of Epitaxial Graphene

Raman Spectroscopy was used to determine the number of graphene layers. Atomic Force Microscopy was used to define the nanotribological properties of the samples. Before the AFM measurements, AFM tips were calibrated because the cantilever properties (dimensions, material properties, etc.) effect friction force measurements on samples.

3.3.1. Raman Spectroscopy

Raman spectroscopy is a spectroscopic technique which is used to observe rotational, vibrational and other low-frequency modes for analysis of a wide range of samples.[34] It was discovered by an Indian physicist Sir Chandrasekhara Venkata Raman. It settles most of the restrictions of other spectroscopic methods. It can be utilized for both qualitative and quantitative purposes. Qualitative analysis can be measured by the frequency of scattered radiations whereas quantitative examination can be performed by measuring the intensity of scattered radiations.

A Raman Spectroscopy can be classified into two parts as seen in Figure 13 . Input system which beam expander, Rayleigh filters, excitation source and focusing mirror. Excitation source generates input rays and this creates excitation in sample. This causes Raman effect. The input rays passes through the beam expander to develop the beams after going to Rayleigh filters. These Rayleigh filters are used to focus mirror rays in

order to transport the rays to the sample solution. Output system consists of focusing mirror, gratings, Rayleigh filters, focusing mirror, detector[35].

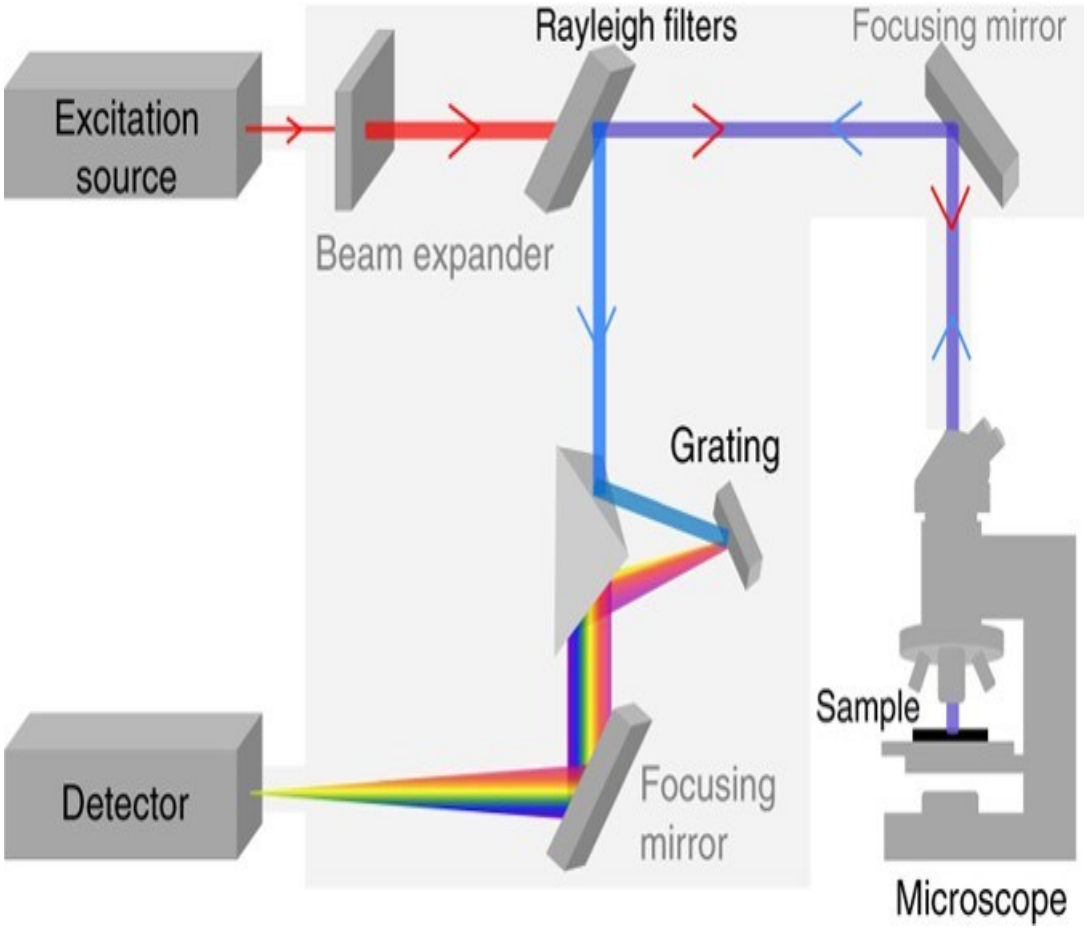

Figure 13. Raman Spectroscopy system[35]

Output rays which are reflected from sample is focused to Rayleigh filter. This filter will block the laser line (Rayleigh scatter) while allowing the Raman scattered light through to the spectrometer and detector. This means some of output rays have same wavelength. Filtered light will goes to gratings for splitting light into several beams. This splitted beams will be focused to detector by focusing mirror. A detector which is very sensitive to light will produce spectrum data named Raman spectra. This spectrum can be produced that showing the intensity of the exiting radiation for each varying frequency of the radiation. This spectrum will show which frequencies of radiation have been absorbed by the molecule to raise it to higher vibrational energy states. When the light hits a substrate, it is excited and is forced to vibrate and move. These vibrations that we are measuring gives the characteristic Raman peaks of the substrate[35].

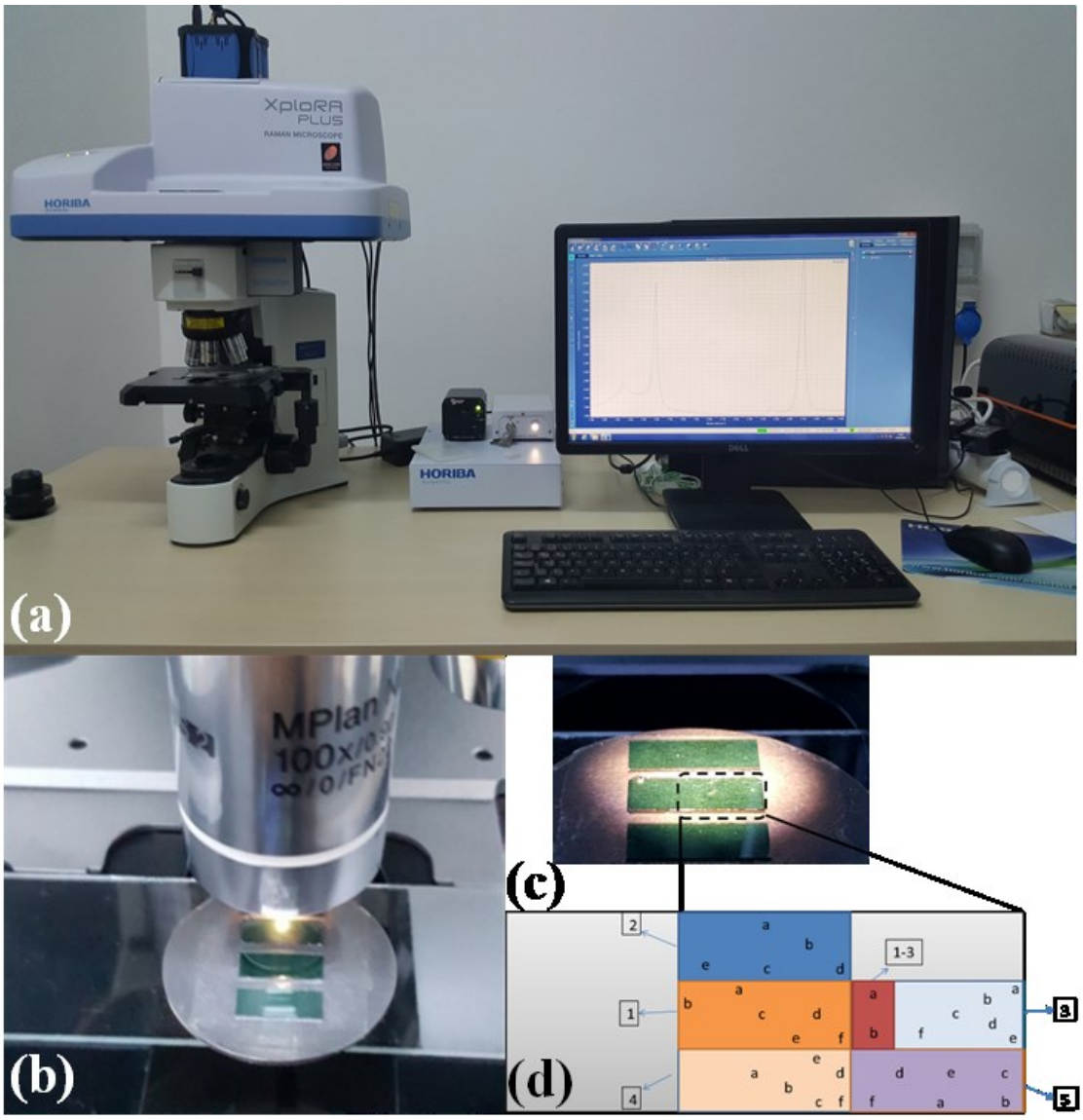

Figure 14. (a) Raman spectrometer set-up (b) SiC samples under the Optical Microscope of Raman Spectrometer (c) SiC samples (d) The regions and points of which Raman Spectroscopy measurements.

In short, Raman Spectroscopy measurements have crucial importance for layer characterization of our graphene substrate. As mentioned before, Raman measurements are required for the ensuring of layer characterization. Basically graphene has three characteristic peaks for defining the structural properties of itself which are called D, G and 2D bands. The G band appears around 1587 cm^{-1} in the spectrum of graphene. This band is an in-plane vibrational mode which gives information us that sp^2 hybridized carbon atoms and the number of layers of graphene. D band represents the defects on graphene sheet which appears around 1350 cm^{-1}. The defect concentration has an important role because it may effect the friction force measurements.

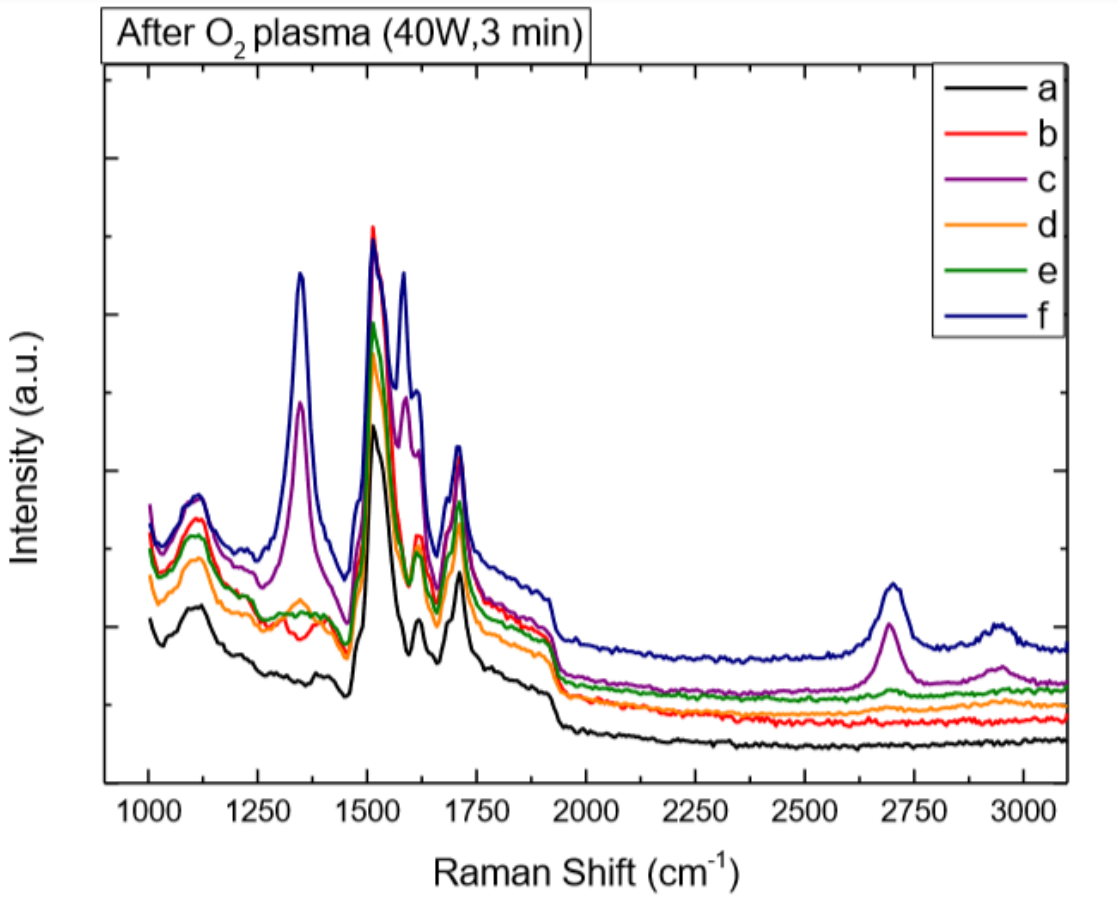

Figure 15. Raman Spectroscopy measurements of graphene grown on the C-face of SiC taken from the Region 4-e for single layer graphene grown on the C-face and Region 4-c for multilayer grown on the C-face

Single layer graphene can also be identified by analyzing the peak intensity ratio of the 2D and G bands. 2D band which appears ~2707 cm^{-1}, a second-order overtone of a different in-plane vibration. Generally, the ratio I_{2D}/I_G of these bands for high quality single layer graphene will be seen to be equal to 2. This ratio, lack of a D band and a sharp symmetric 2D is often used as a confirmation of high quality defect free graphene sample. The strong G peak and the weak D peak indicate good graphitic quality[33]. Also the D to G peak intensity ratios (I_D/I_G) for multilayer graphene is higher than that the ratio of the single layer graphene[36] .

The graphene layers on both Si-face and C-face of SiC were analyzed by Raman Spectroscopy measurements at IZTECH. As seen in Figure 14 , our samples were placed under the Raman Spectroscopy microscope. The points a, b, c, d, etc. display that Raman measurements were taken from these points. For the characterization, two regions were chosen for each friction measurements, these regions were scanned for 3 times.

For example, the points in region 2 showed us that we had few and multilayer graphene grown on the C-face SiC sample. On the contrary, monolayer graphene was detected on the region 4-c and 4-e as shown in Figure 15 . Therefore AFM measurements were taken from the points c (multilayer) and e (single layer) which were identified by Raman Measurements as can be seen in Figure 15 .

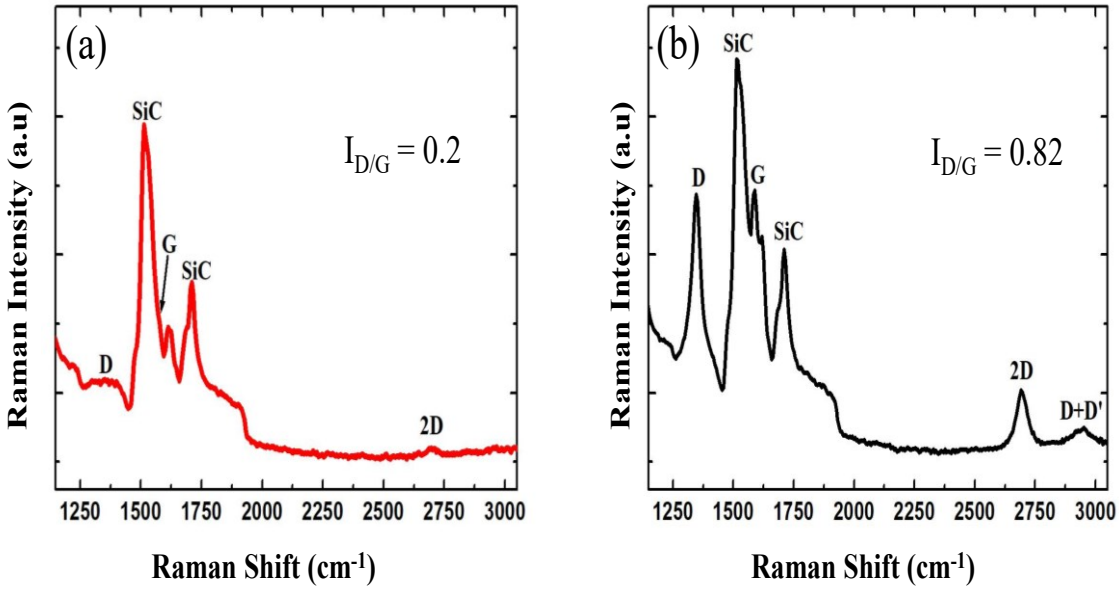

Figure 16. (a) Raman peaks of single and (b) multi-layer graphene grown on SiC

As can be seen in Figure 16 , multi-layer graphene and single layer graphene comparison have also been studied. When looking at these Raman spectra in Figure 16 , in multi-layer graphene, 2D peak is much intensive compared to the single layer graphene as the number of layers is increased. As same manner, in the single layer graphene, the SiC peak is much stronger than the G peak and this proved us that single layer graphene has obtained.

For each analysis, the intensity ratio of the D over G was calculated. The difference in this ratio gives us the defect concentration of the graphene grown on the single layer and multi-layer graphene. Single layer graphene has the ratio of 0.2 while multi-layer graphene has 0.82.

When we look closer to the Raman peaks of the single and multilayer graphene grown on the C-face of SiC, characteristic peaks are D (1346.81 cm^{-1}) which shows the defect, G (1571.9 cm^{-1}) which is important for identifying the number of graphene layers

that can be called graphitic peak and 2D (2687.1 cm^{-1}) peak which comes from the in-plane modes for single layer graphene grown on C-face.

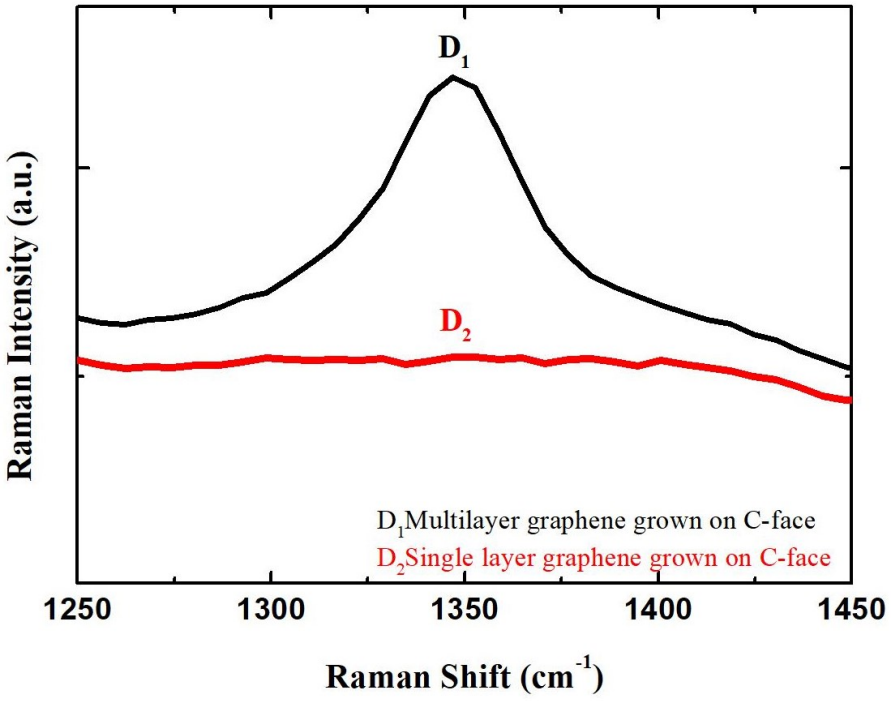

Figure 17. The intensity of D peaks of single and multilayer graphene grown on C-face

These values are D (1346.81 cm^{-1}), G (1589.41 cm^{-1}) and 2D (2692.18 cm^{-1}) for the multilayer graphene grown on C-face. D peak intensity of multilayer is higher than that of the single layer graphene on the C-face of SiC as shown in Figure 17 .

The samples were identified as monolayer and multi-layer graphene, then they were ready to be analyzed with AFM as mentioned in Chapter 3.3.2.

3.3.2. AFM Measurements

AFM is the most commonly used instrument in all scanning probe microscopes. Nowadays, AFM is used by researchers to determine properties of materials such as surface topography, adhesion, friction, wear, lubricity of films and mechanical measurement [37] ranging from one micrometer to nanometer scale lubricant molecules or other semiconducting materials.

AFM was a development of Scanning Tunneling Microscopy (STM)[38]. STM was an instrument which was invented by Binnig and Rohrer had much higher resolution than the topografiner that is similar but earlier invention, as it monitored electron tunneling, typically from one atom at the end of a probe to a conducting substrate. However, both techniques were limited in what samples could be analyzed. Hence, Binnig, Quate and Gerber replaced the electron tunneling from a wire of the STM with the cantilever of

AFM, and they succeeded to analyze insulating samples, after that there have been lots of developments and new modes of operation devised for AFM[38].

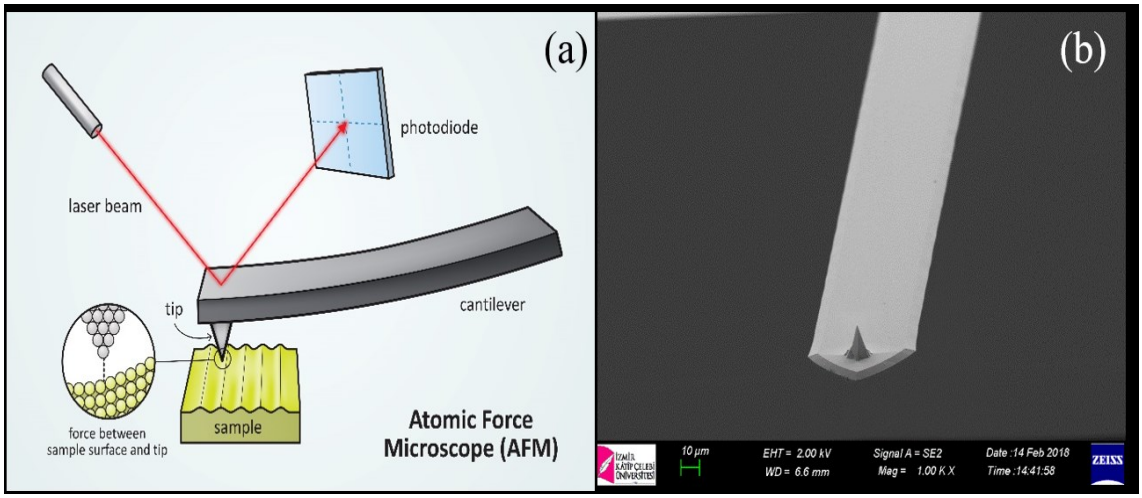

Figure 18. (a) Basic principle of AFM and (b) SEM image of our AFM (PPP-XYCONTR) cantilever

The basic principle of AFM is that a probe is maintained very close to the sample surface by a feedback mechanism. As the AFM tip scans over the surface, the feedback mechanism helps the movement of the probe to stay at the same probe-sample distance and it gives the sample topography. There are lots of probes to be used but the most commonly used are micro-fabricated silicon (Si) or silicon nitride (Si_3N_4) cantilevers with integrated tips. The tips can be very sharp and we used AFM tip which was suitable for the friction force measurements of the samples.

The bending of the cantilever normal to the sample surface is usually monitored by an optical lever[38]. The AFM system[39] magnifies the normal bending of the cantilever greatly, and is sensitive to Angstrom-level movements. There are several modes of scanning but for the friction measurement, we used contact mode AFM that the probes touches the sample as it moves over the surface. The movement of the probe over the

surface is controlled by a scanner. A scanner made from a piezoelectric material which can move the probe very precisely in the x, y, and z directions. From the photodetector, the signal passes through a feedback mechanism, and the z-movement of the scanner, in order to maintain the probe-sample distance at a set value. In AFM, cantilever can be thought as a spring. The distance by which the scanner has to move in the z axis to maintain the cantilever deflection which is taken to be equivalent to the sample topography. During contact-mode scanning, the amounts of deflection and torsion that is obtained when the laser beam hits to the sample. The laser reflects from the backside of the cantilever and strikes to the four quadrants photodiode (A, B, C, D) as can be seen in Figure 18 .

For the FFM measurements, the quantitative determination of friction forces by AFM requires the conversion of the output voltage signal of the sector area-sensitive photodiode to force. At the end, the friction force was calculated by multiplying the lateral deflection signal (V) and calibration constant (α).

Cantilever deflects vertically due to the normal interaction forces (F_N) acting between the probe and sample and twists due to the lateral interaction forces (F_L). The determination of the differential voltage signal intensity from the top (A and B) and bottom (C and D) quadrants of the photodetector is necessary for the measurement of the normal load between the probe and sample. There is a linear relationship between the differential voltage signal intensity from the top and bottom parts of the photodetector ((A+B)-(C+D)) and the normal load F_N as can be seen in Equation 3.3.2.1 below[40].

$$F_N = \{\alpha [(A + B) - (C + D)]\} \quad (3.3.2.1)$$

As the same manner, the voltage signal intensity difference between the left (A and C) and right (B and D) quadrants of the photodetector gives the information about the lateral force F_L. The lateral force is linearly proportional to the differential voltage signal intensity from left and right quadrants, as can be seen in Equation 3.3.2.2 below[40,41]:

$$F_L = \{\mu [(A + B) - (C + D)]\} \quad (3.3.2.2)$$

Equation 3.3.2.2 gives us μ is the lateral force calibration factor. While scanning the surface back and forth voltage signals gives us a friction loop (see Figure 19) in terms

of voltage units. The data which comes from this friction loops were converted into force units in order to find the correlated graph of friction force versus applied load on the sample at the end[6].

Our AFM set-up which has a micro stage to operate precisely is shown in Figure 20 . Generally there are three main parts are important while operating AFM: Z-motor, AFM head which has photodiode and piezoelectric components to operate AFM and Controller. Sample can be placed onto the sample holder at the sample stage which can be seen in Figure 20 .

To conduct the AFM measurements, first the laser spot is adjusted at the center of the four quadrant photodetector in order to take the initial values of F_L and F_N zero. Nevertheless, this adjustment may be shifted during the measurements due to thermal drift or a coupling between the deflection and torsional twisting experienced by the cantilever. In order to eliminate this problem for a well-calculated lateral force data, friction force (F_f) values are always calculated for each measurements.

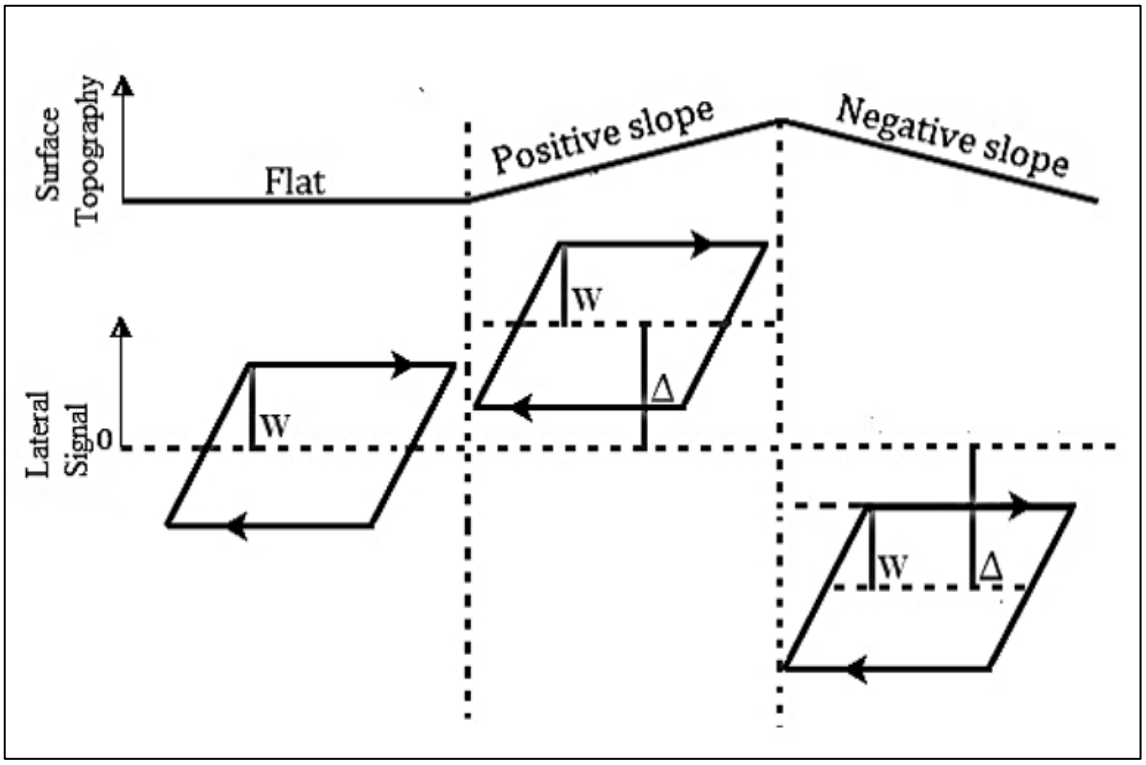

Figure 19. The schematics of friction loops (lateral signals for back and forth scans) for flat, positively sloped and negatively sloped surfaces at the same applied load by taking the half-width of friction loops were obtained by lateral forces recorded during back and forth scanning of the same scanned area)[42].

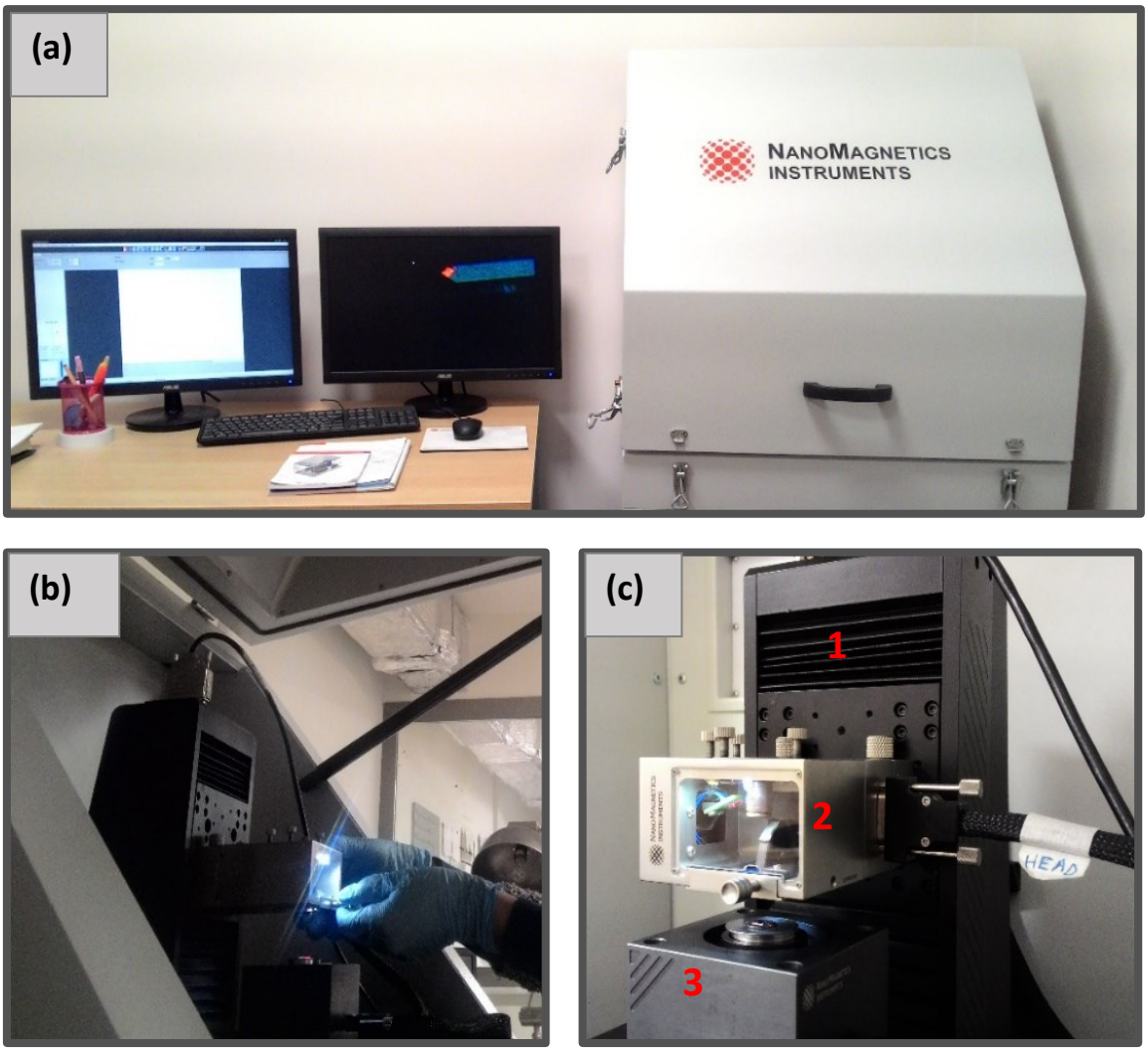

Figure 20. (a) Atomic force microscope (b) Cantilever and sample installment (c) 1-Z motor 2- AFM head 3-Sample stage

We conducted friction force measurements on the single and multilayer graphene grown on C-face of SiC by using AFM tip (PPP-XYCONTR) and as well as the friction force measurement comparison of the single layer graphene grown on Si-face and C-face with small and bigger loads (0.5 nN - 5 nN) and (10 nN - 40 nN).

CHAPTER 4

FRICTION FORCE MEASUREMENTS

4.1. Calibration of AFM Cantilevers

Frictional properties of our samples were measured by using NanoMagnetics [43] Ambient AFM system with contact mode. Initially, AFM cantilevers were calibrated by scanning the trapezoidal shaped of test grating samples which was mentioned in Varenberg's study (TGF11 by MikroMasch, see Figure 21).

AFM is a way of defining quantitative measurement of contact response, it requires complex calibration of both normal and lateral forces of cantilever[6]. After G. Binning and H. Rohrer invented AFM and won the Nobel Prize in 1986[44,45], friction measurements at atomic scale single asperity geometries have been performed by lots of scientists[46]. It is relies on detection of atomic scale interaction forces between a sample and a sharp tip for imaging.

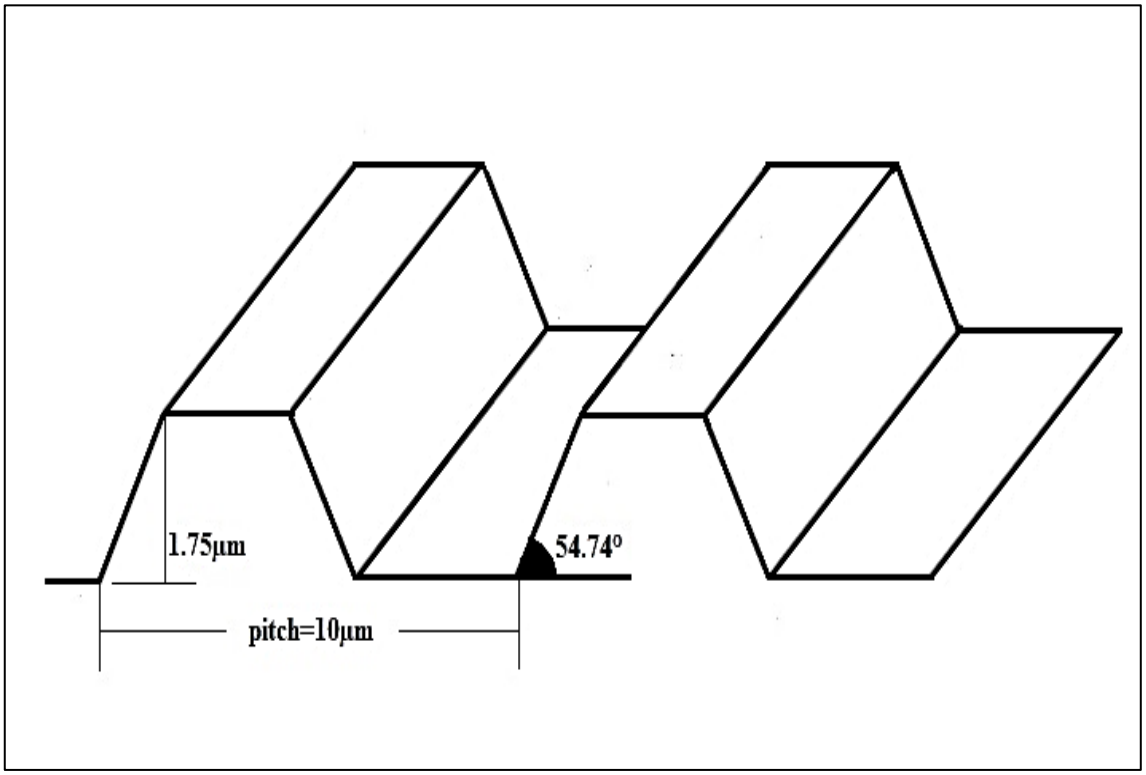

Figure 21. Trapezoidal shape of test grating sample for calibration, TGF11 (MicroMasch)

Generally contact mode AFM is used to analyze the friction force coefficient of surfaces. Basically while analyzing the lateral friction measurements, two steps must be carried out. One is calibration of cantilevers to sense the desired surface by AFM to find the increased applied loads on surface for our measurements. Firstly, Sader Method[7] was used for calibration of AFM tips in order to find the k spring constant. The normal spring constants of rectangular cantilevers were used. The determination of the resonance frequency and mass of the cantilever is related to the cantilever calibration. For this reason the normal spring constant of rectangular cantilever which were used in our experiments was calculated by:

$$k = \rho bhLM_e\omega^2{}_{vac} \tag{4.1}$$

where ρ is the density of the cantilever (for Si, 2.329 g/cm^3), b, h, and L are the width (50 µm, thickness (2 µm) and length of the cantilever (450 µm). In this Equation 4.1[7], M_e is the effective mass and the spring constant of the AFM cantilever was found as 0.1474 N/m so the aspect ratio of the cantilever (L/b) is higher than 5. The value of ω_{vac} is the angular resonance frequency of the cantilever in vacuum.

After that Ogleetre method to find the calibration factor and friction coefficient values: α and µ of the cantilevers[42]. For the calibration of cantilevers, trapezoidal test grating samples[47] were used to find these values shown in Equation 4.2 and 4.3 below. After these two steps, the lateral forces are recorded while scanning the sample surface with respect to applied loads.

In the following equations, once W' and D' can be found from the slope of the back and forth signals, µ can be determined. Here, θ represents the angle of the inclined surface of trapezoidal test grating sample. Figure 19 represents the schematic friction loops lateral signals for back and forth scans for flat, positively sloped and negatively sloped surfaces at the same applied load. W is the friction loop half-width and D is the friction loop offset. The values of W and D are measured over a range of applied loads for known slopes and used to calibrate the lateral force response of the cantilever. The values of W and D are measured by scanning the trapezoidal shaped test grating sample applying loads for known slopes and used to calibrate the lateral force response of the cantilever[42,47]. The slopes of these plots (W', D') which correspond to the derivative of W and D are put into the following equations that gives force equilibrium arguments.

$$\alpha \times D' = \frac{(1+\mu^2)sin\theta cos\theta}{(cos\theta)^2-\mu^2(sin\theta)^2} \tag{4.2}$$

$$\alpha \times W' = \frac{\mu}{(cos\theta)^2-\mu^2(sin\theta)^2} \tag{4.3}$$

Also in the Sader's and Ogleetre's studies it is mentioned that the dimensions of the cantilever is very important for the calibration of cantilevers. While the back and forth scanning signals gave us the information about the lateral force measurements of the surface, the calibration constant of cantilever was used to convert these signals to nN which describes the friction force on the surface.

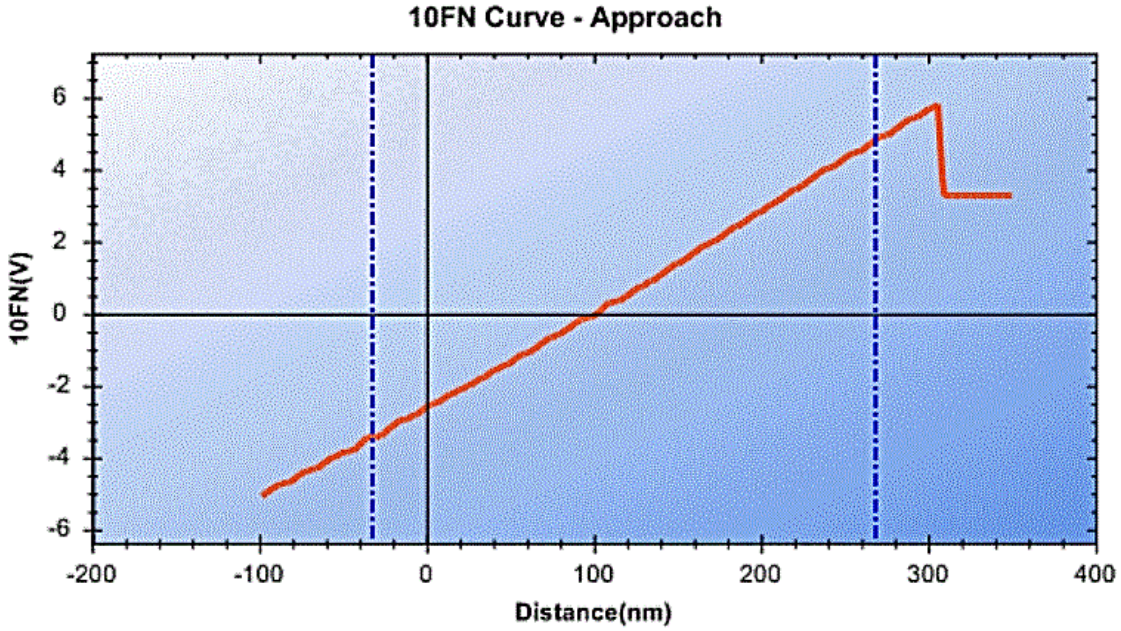

Figure 22. The behavior of the AFM tip while conducting Force Distance (FD) measurements

The desired set voltages which correspond to the applied load were obtained from the FD curve measurements as can be seen in Figure 22 corresponding to lateral forces experienced by the cantilever. The lateral forces recorded on the sloped regions of the grating for each value of the normal load, and for both forward and backward scans that together form friction loops. Subsequently, friction loop half width and friction loop offset

values are determined. These values were plotted with respect to increasing normal load.

The slopes of these plots (W, D) are then put into the Equation 4 and 5 arising from force equilibrium arguments. The spring constant of the PPP-XYCONTR tip has been obtained by employing dynamic mode of the AFM and it has been found as 0.1474 N/m.

Table 3. Set voltage values (V) versus applied load (nN)

Set Normal Value (V)	**Applied Load (nN)**
-1.351	10
-2.090	15
-2.787	20
-3.484	25
-4.200	30
-4.900	35
-5.700	40

Basically while analyzing the lateral friction measurements, two steps were carried out. One was the calibration of cantilever to sense the desired surface by AFM. In order to find the applied loads acting on surface, certain set voltage values must be found (see Table 3) and entered at AFM software.

Table 4. Properties of AFM tip and Scanning Parameters of PPP-XYCONTR

Tip	**PPP-XYCONTR**
k, spring constant	0.1874 N/m
Scan Speed	2.0 µm/s
Scanned Area	(5.0 µm ; 2.5 µm)

The second step was applying these voltages to the mono and multilayer graphene on C-face SiC surfaces to observe the applied load which varies from 10.0 nN to 40.0 nN with an increment of 10.0 nN. After these two steps, the lateral force signals were recorded while scanning the sample surface with respect to applied loads.

The properties of our cantilever which was used to scan the graphene surface can be seen in the Table 4 .

The sample's scanned area was (5.0 µm; 2.5µm) and the scanning speed was set as 2 µm/s. The scan speed is important because of while scanning, the thermal drift and noise may easily occur and affect our friction measurements.

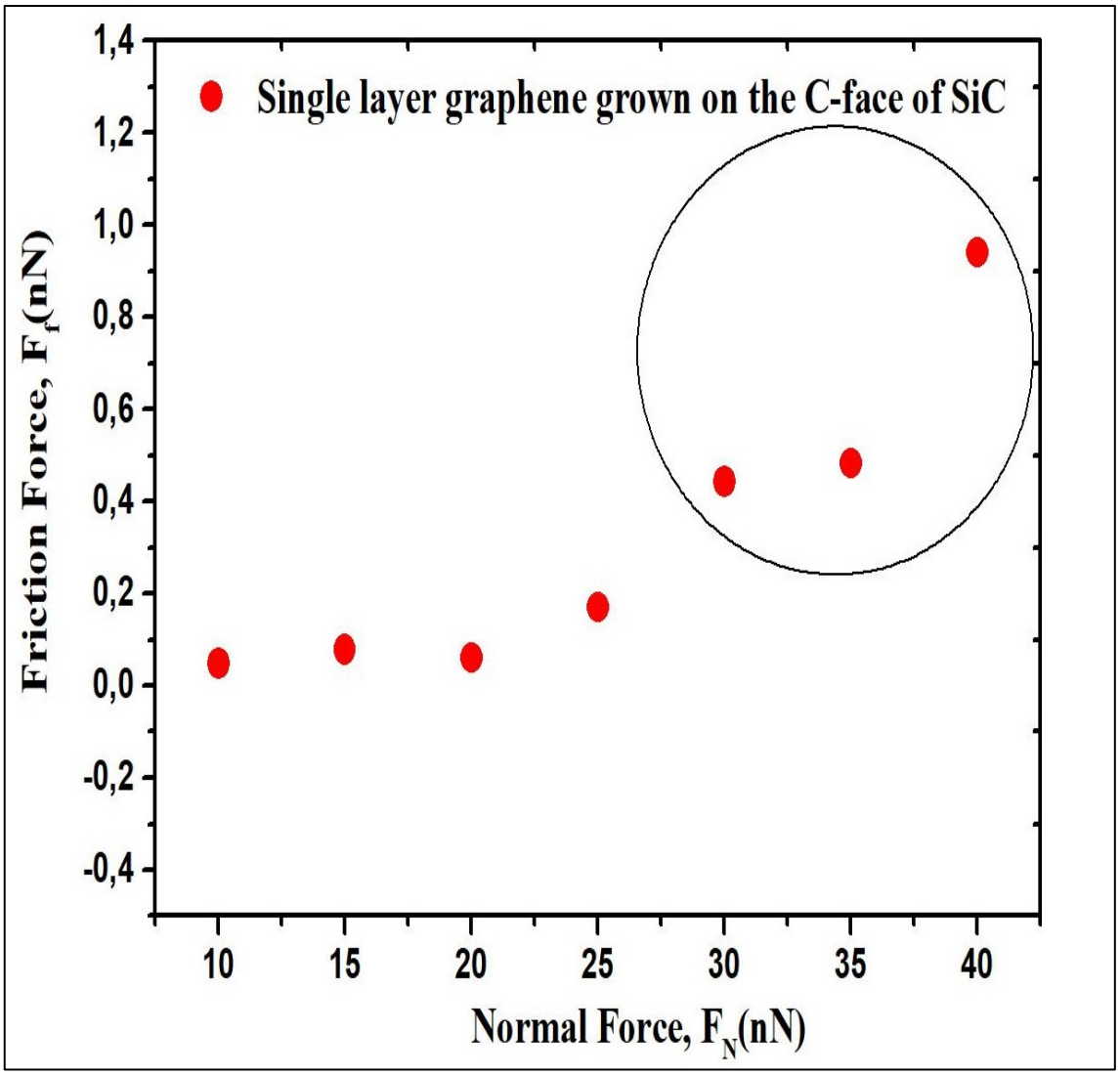

Figure 23. Single layer graphene grown on the C-face of SiC

4.2. Friction Force Measurements by using AFM

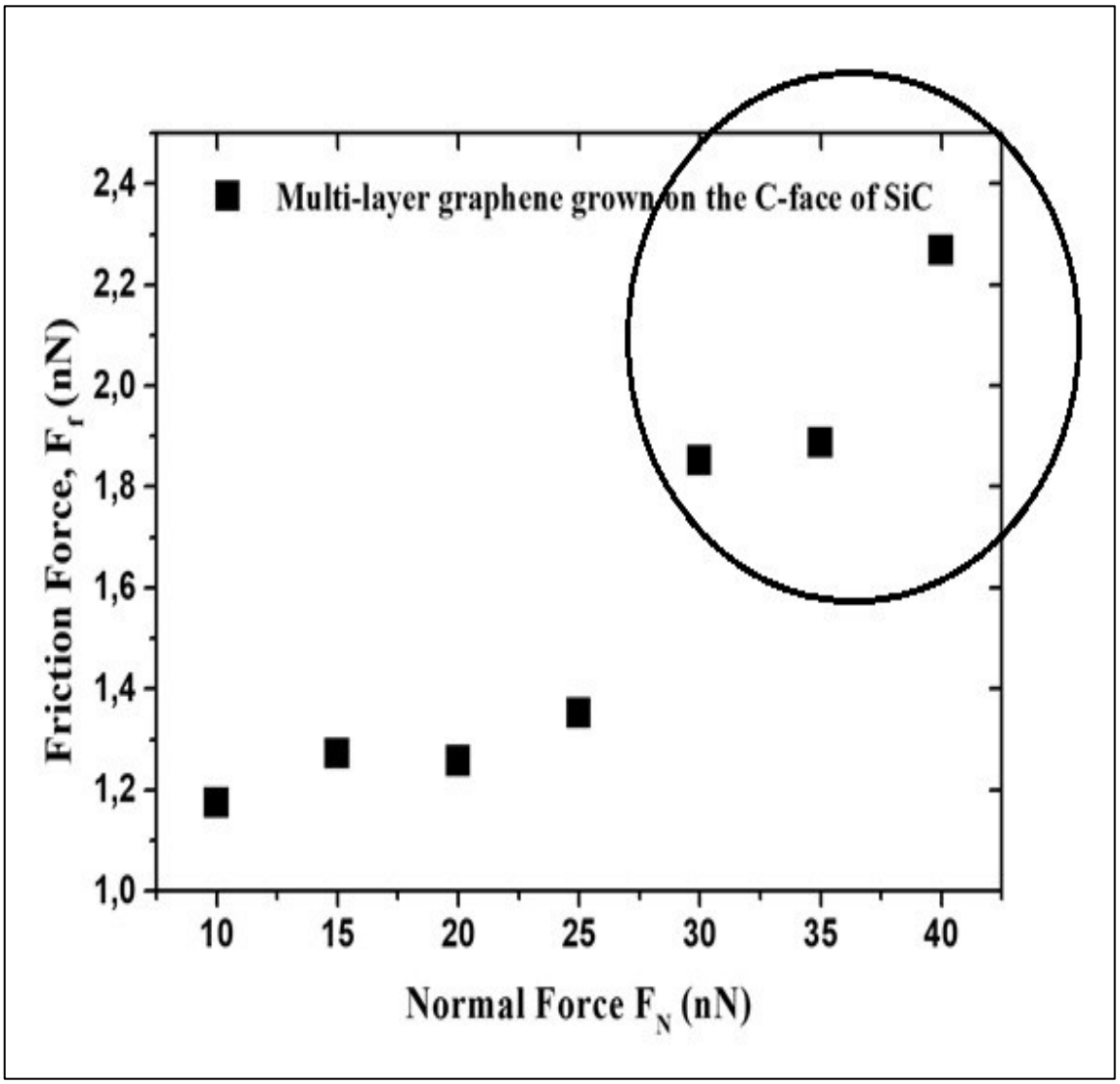

Figure 24. Multilayer Graphene Grown on the C-face of SiC

In this thesis the friction force of epitaxial graphene have been investigated for both Si-face and C-face of SiC. Dependence of friction force on single and multi-layer graphene were studied on this study to see the thickness-dependence of C-face of SiC.

As can be seen in Figure 23 and Figure 24 This is caused by the working interval of AFM tip. Beyond this value, the linearity broke down and exponential increase

occurred on both C-face and Si-face for each measurements. The reason behind this was tip deflection and it may be attributed as artifact.

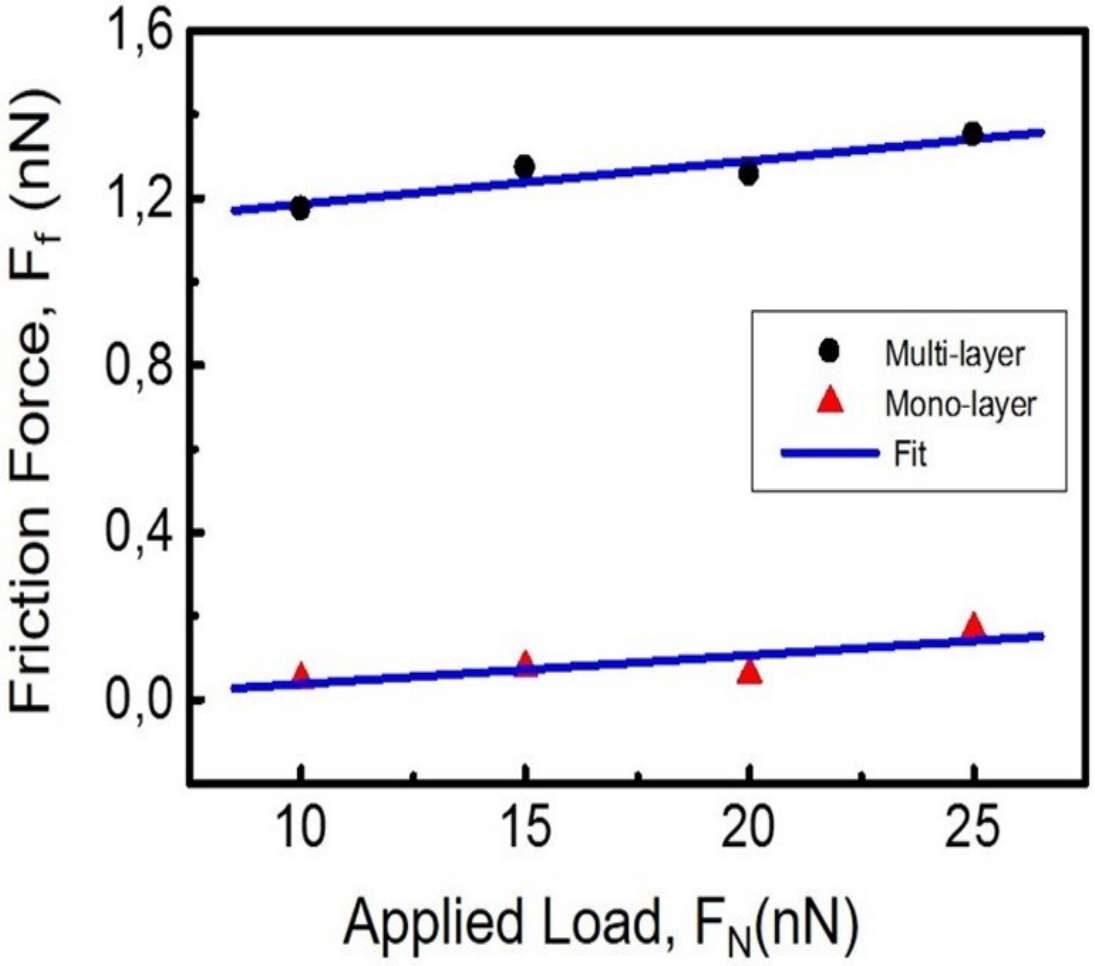

Figure 25. Friction force measurements of mono-layer (red triangles) and multi-layer (black dots) graphene grown on the C-face of SiC

As can be seen in the Figure 25 , single layer graphene grown on the C-face showed less friction rather than multi-layer graphene on the C-face of SiC. When the number of graphene layer were increased, the friction force on graphene increased too. According to these results, our measurements showed that the friction force of single layer graphene is lower than the multi-layer graphene in Figure 25 . The friction coefficients of single layer graphene and multilayer graphene grown on the C-face of SiC was found as 0.02 and 0.82 respectively. As mentioned before, the difference in the friction coefficients

of the multi-layer and single layer graphene gives us the tribological properties of graphene.

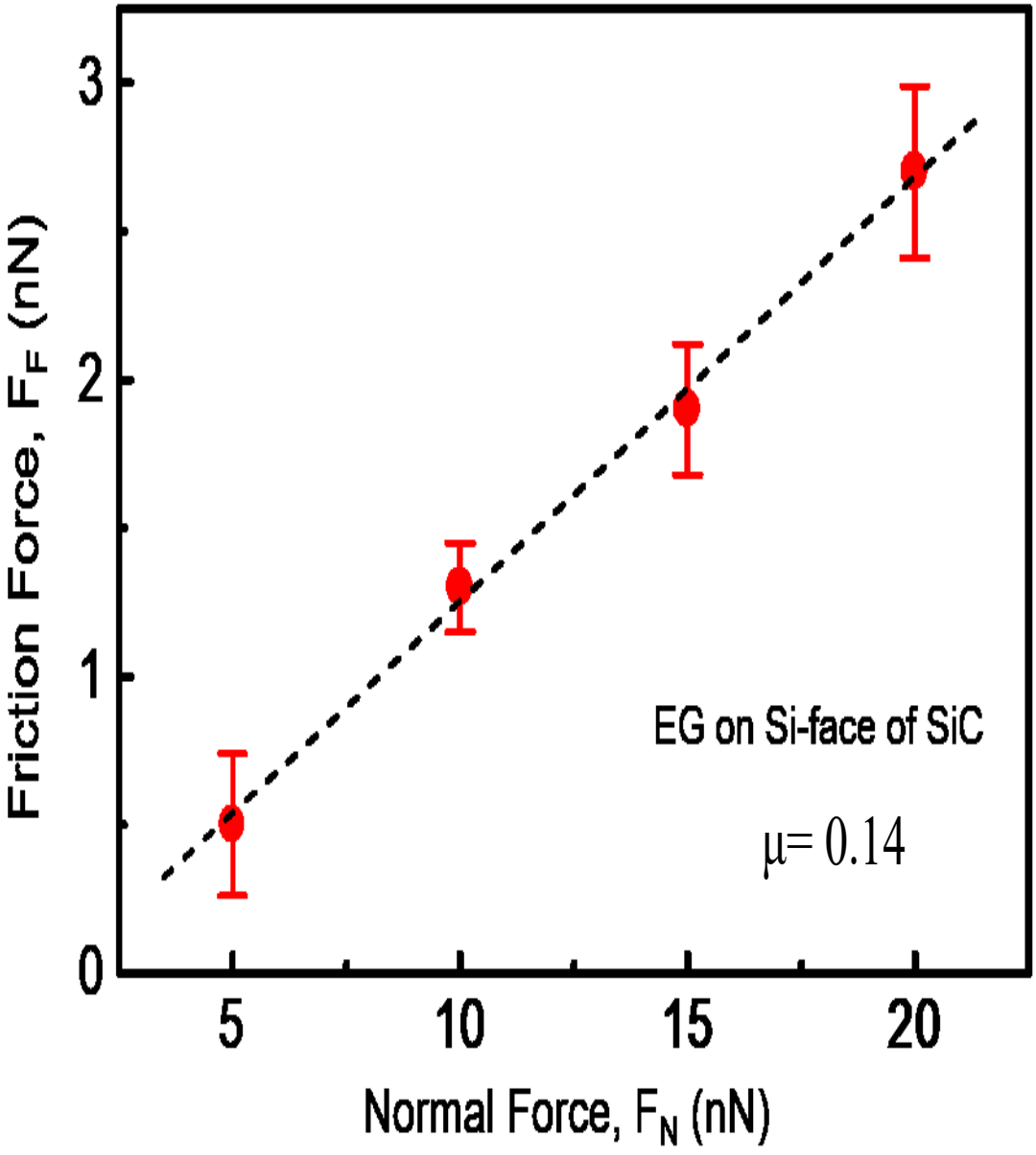

Figure 26. Friction force measurement of EG on Si-face of SiC substrate

The friction measurements of the single layer graphene grown on both C-face and Si-face were compared by the AFM (see in Figure 26 and Figure 27). In this comparison, single layer graphene grown on the C-face has lower friction coefficient compared to the Si-face of SiC. This means friction is lower in single layer graphene grown on the C-face than that on the Si-face of SiC. As mentioned before there is no interface layer between

the graphene layer and SiC. This may be caused by the weak interaction between SiC and graphene layer on the C-face of SiC.

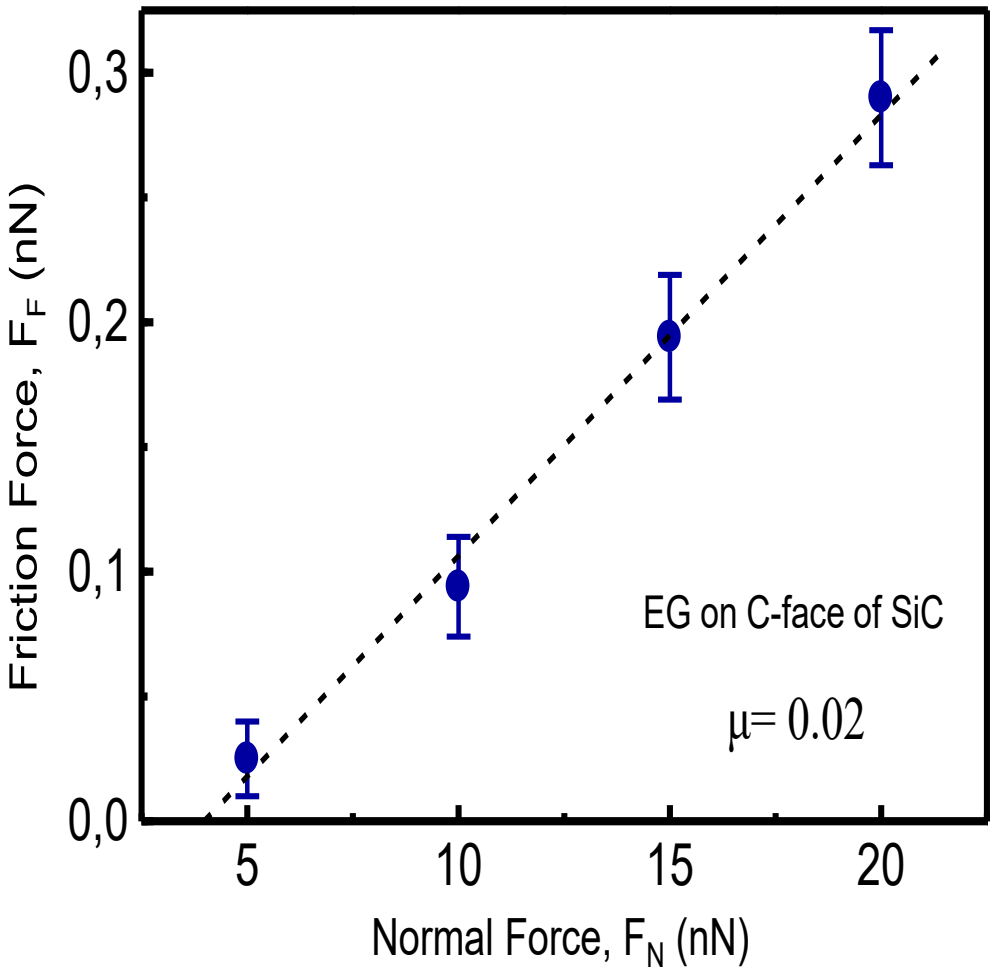

Figure 27. Friction force measurement of EG on C-face of SiC substrate

The comparison between the single layer graphene on both C-face and Si-face of SiC semiconductor in the range between 5.0 nN to 20 nN with 5.0 nN increment showed that the friction force (F_F) due to the applied load ($F_{applied}$) the friction coefficient of graphene grown on the Si-face of SiC is higher than the friction coefficient of graphene grown on the C-face. The coefficient of friction values for Si-face and C-face are 0.14 and 0.02 respectively.

In addition to these results before and after SEM measurements of the AFM cantilever that we conducted in this experiment, for the bigger loads on the sample were

shown in Figure 28 . The tip which was contact with the surface the tip became blunt after several times.

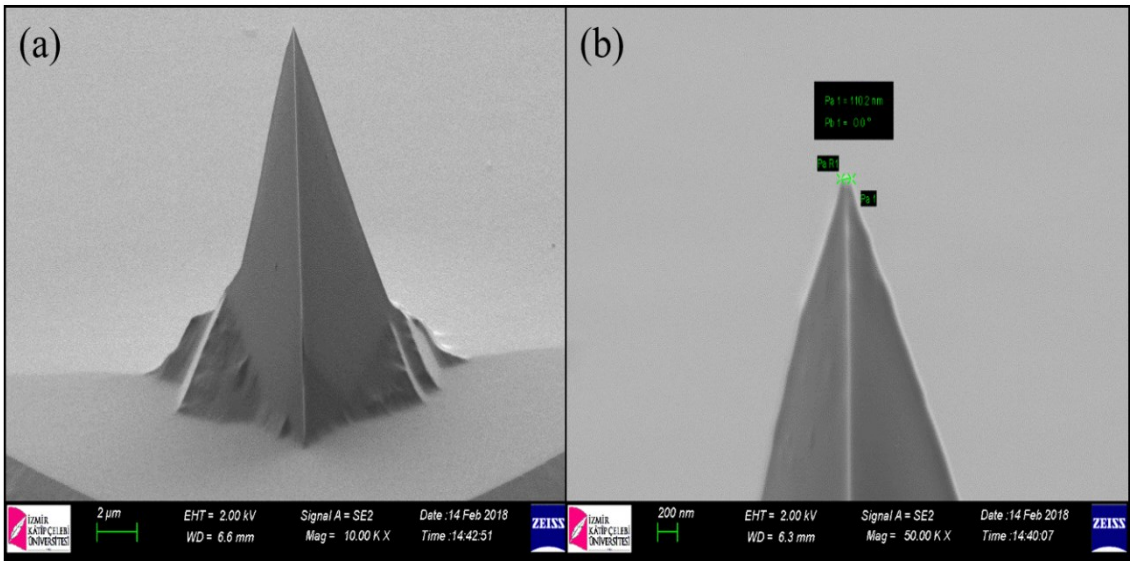

Figure 28. Scanning Electron Microscopy images of AFM cantilever (a) before use (b) after friction force measurements

CHAPTER 5

CONCLUSION

In this master thesis, a compherensive characterization of nanotribological properties of epitaxial graphene grown on SiC has been presented by using AFM. To analyze nanotribological properties of epitaxial graphene grown on SiC, friction coefficients of single layer graphene grown on the Si-face and the C-face and friction coefficients of single and multi-layer graphene grown on the C-face of SiC have been investigated.

Scanning the surface with an applied force from 5.0 nN to 40 nN with a 5.0 nN increment and obtaining the friction force (F_F) due to the applied load ($F_{applied}$) helped us to see the trend of the friction behavior of graphene. The results showed different friction coefficients but same trend as they both increase linearly. However the trend is consistent with other studies, applied load above the 20 nN, AFM cantilever was effected from the tip deflection. It can be also seen that the friction force occurs even at the zero applied normal load which gave us an offset for each measurements. This is attributed to the intrinsic or initial adhesion force due to the attractive forces such as capillary, electrostatic force between tip and the sample. Because the FFM measurements were conducted in ambient conditions, the existence of water from the environment is the origin of the capillary force with respect to hydrophilic nature of the surface.

When we compared the single layer graphene grown on the Si-face and C-face of SiC substrate showed that single layer graphene grown on the C-face has lower friction coefficient compared to the Si-face of SiC substrate.

Raman spectroscopy were conducted to determine the number of graphene layers and the amount of defects associated with these grown layers. Raman spectroscopy measurements showed that the amount of defects in multi-layer graphene is greater than that of mono-layer graphene. Following Raman measurements the graphene layers were characterized by AFM in order to reveal their surface friction properties. The results of AFM measurements showed that the coefficient of friction for multilayer graphene is about two time greater than the one measured for mono-layer epitaxial graphene. The difference in friction coefficients were attributed to the amount of defects identified for

both samples. As the D defect peak intensity was increased in multilayer graphene which may resulted from the dislocations, corrugation and interaction of layers and the grain boundaries, the friction of multilayer graphene increased too. This may be caused by the wave functions of defects on each layers in multilayer graphene.

As a result, single and multi-layer graphene samples were grown on the C- face of SiC. As results that were shown in multilayer graphene grown on the C-face of SiC substrate SiC was more defective rather than the single layer graphene grown on the C-face of SiC substrate.

Lastly, graphene can be a good candidate for reducing friction on SiC which can be technologically used as a low-friction anti wear coating. These results contribute to investigation of graphene tribology at the micro and nanoscale applications in future.

Furthermore, when these new results are supported by theoretical results, this may leads new developments in many applications.

REFERENCES

1. Bhushan, B. *Handbook of micro/nano tribology*. *Mechanics and materials science* (1995). doi:10.1201/9781420050493

2. Jost, H. P. *Lubrication: Tribology; Education and Research; Report on the Present Position and Industry's Needs (submitted to the Department of Education and Science by the Lubrication Engineering and Research) Working Group*. (HM Stationery Office, 1966).

3. Holscher, H., Schirmeisen, A. & Schwarz, U. D. Principles of atomic friction: from sticking atoms to superlubric sliding. *Philos. Trans. R. Soc. A Math. Phys. Eng. Sci.* **366,** 1383–1404 (2008).

4. Geim, A. K. & Novoselov, K. S. The rise of graphene. *Nat. Mater.* **6,** 183–191 (2007).

5. Berman, D., Erdemir, A. & Sumant, A. V. Few layer graphene to reduce wear and friction on sliding steel surfaces. *Carbon N. Y.* **54,** 454–459 (2013).

6. Varenberg, M., Etsion, I. & Halperin, G. An improved wedge calibration method for lateral force in atomic force microscopy. *Rev. Sci. Instrum.* **74,** 3362–3367 (2003).

7. Sader, J. E. *et al.* Calibration of rectangular atomic force microscope cantilevers Calibration of rectangular atomic force microscope cantilevers. *Rev. Sci. Instrum.* **3967,** 1–4 (1999).

8. Izhevskyi, V. A., Genova, L. A., Bressiani, J. C. & Bressiani, A. H. A. Review article: silicon carbide. Structure, properties and processing. *Cerâmica* **46,** 4–13 (2000).

9. Li, X. *Epitaxial graphene films on silicon carbide: Growth, characterization, and devices*. (Georgia Institute of Technology, 2008).

10. Maruyama, T. & Naritsuka, S. Initial Growth Process of Carbon Nanotubes in Surface Decomposition of SiC. in *Carbon Nanotubes - Synthesis, Characterization, Applications* 29–46 (2011). doi:10.5772/978

11. Han, Y., Aoyama, T., Ichimiya, A., Hisada, Y. & Mukainakano, S. Atomic models of ($\sqrt{3}\times\sqrt{3}$)R30° reconstruction on hexagonal 6H–SiC(0001) surface. *J. Vac. Sci. Technol. B Microelectron. Nanom. Struct.* **19,** 1972 (2001).

12. Verma, A. R. & Krishna, P. Polymorphism and polytypism in crystals. *1966, 341 P. JOHN WILEY SONS, INC., 605 THIRD Ave. NEW YORK, N. Y. 10016* (1965).

13. Schneer, C. J. Polymorphism in one dimension. *Acta Crystallogr.* **8,** 279–285 (1955).

14. de Heer, W. A. *et al.* Large area and structured epitaxial graphene produced by confinement controlled sublimation of silicon carbide. *Proc. Natl. Acad. Sci.* **108,** 16900–16905 (2011).

15. Jernigan, G. G. *et al.* Comparison of epitaxial graphene on si-face and C-face 4H

SiC formed by ultrahigh vacuum and RF furnace production. *Nano Lett.* **9,** 2605–2609 (2009).

16. Rutter, G. M. *et al.* Imaging the interface of epitaxial graphene with silicon carbide via scanning tunneling microscopy. *Phys. Rev. B - Condens. Matter Mater. Phys.* **76,** 1–6 (2007).

17. Riedl, C., Starke, U., Bernhardt, J., Franke, M. & Heinz, K. Structural properties of the graphene-SiC(0001) interface as a key for the preparation of homogeneous large-terrace graphene surfaces. *Phys. Rev. B - Condens. Matter Mater. Phys.* **76,** (2007).

18. Emtsev, K. V., Speck, F., Seyller, T., Ley, L. & Riley, J. D. Interaction, growth, and ordering of epitaxial graphene on SiC{0001} surfaces: A comparative photoelectron spectroscopy study. *Phys. Rev. B - Condens. Matter Mater. Phys.* **77,** (2008).

19. Bhushan, B. *Modern Tribology Handbook Volume One Principles of Tribology*. *CRC press LLC* (2001). doi:10.1016/S0301-679X(02)00259-1

20. Demirbaş, T. & Baykara, M. Z. Nanoscale tribology of graphene grown by chemical vapor deposition and transferred onto silicon oxide substrates. *J. Mater. Res.* **31,** 1914–1923 (2016).

21. Hass, J. *et al.* Why Multilayer Graphene on $4\,H-SiC\,(000\,\bar{1})$ Behaves Like a Single Sheet of Graphene. *Phys. Rev. Lett.* **100,** 125504 (2008).

22. Filleter, T. & Bennewitz, R. Structural and frictional properties of graphene films on SiC(0001) studied by atomic force microscopy. *Phys. Rev. B* **81,** 155412 (2010).

23. Huang, F., Li, K. & Kulachenko, A. Measurement of interfiber friction force for pulp fibers by atomic force microscopy. *J. Mater. Sci.* (2009). doi:10.1007/s10853-009-3506-8

24. Maboudian, R. Critical Review: Adhesion in surface micromechanical structures. *J. Vac. Sci. Technol. B Microelectron. Nanom. Struct.* (1997). doi:10.1116/1.589247

25. Filleter, T. *et al.* Friction and dissipation in epitaxial graphene films. *Phys. Rev. Lett.* **102,** (2009).

26. Van Bommel, A. J., Crombeen, J. E. & Van Tooren, A. LEED and Auger electron observations of the SiC(0001) surface. *Surf. Sci.* **48,** 463–472 (1975).

27. De Heer, W. A. *et al.* Epitaxial graphene electronic structure and transport. *J. Phys. D. Appl. Phys.* **43,** (2010).

28. Hass, J. *et al.* Why multilayer graphene on 4H-SiC(000$\bar{1}$) behaves like a single sheet of graphene. *Phys. Rev. Lett.* **100,** (2008).

29. Çelebi, C., Yanık, C., Demirkol, A. G. & Kaya, İ. İ. The effect of a SiC cap on the growth of epitaxial graphene on SiC in ultra high vacuum. *Carbon N. Y.* **50,** 3026–3031 (2012).

30. Tedesco, J. L. *et al.* Hall effect mobility of epitaxial graphene grown on silicon carbide. *Appl. Phys. Lett.* **95,** (2009).

31. Mallet, P. *et al.* Electron states of mono- and bilayer graphene on SiC probed by scanning-tunneling microscopy. *Phys. Rev. B - Condens. Matter Mater. Phys.* **76,** (2007).

32. Hass, J., De Heer, W. A. & Conrad, E. H. The growth and morphology of epitaxial multilayer graphene. *Journal of Physics Condensed Matter* **20,** (2008).

33. Lin, Z. *et al.* Precise control of the number of layers of graphene by picosecond laser thinning. *Sci. Rep.* **5,** (2015).

34. Gardiner, D. J. Introduction to Raman Scattering. in *Practical Raman Spectroscopy* 1–12 (1989). doi:10.1007/978-3-642-74040-4_1

35. Raman spectroscopy. Available at: http://way2science.com/raman-spectroscopy-2/.

36. Ni, Z. H. *et al.* Raman spectroscopy of epitaxial graphene on a SiC substrate. *Phys. Rev. B - Condens. Matter Mater. Phys.* **77,** (2008).

37. Bhushan, B. Nanoscale boundary lubrication studies. in *Nanotribology and Nanomechanics: An Introduction: Fourth Edition* 689–746 (2017). doi:10.1007/978-3-319-51433-8_14

38. AFM: Beginner's Guide. *2018 AFMHelp.com* Available at: http://afmhelp.com/index.php?option=com_content&view=article&id=51&Itemid=57.

39. http://www.nisenet.org/catalog/scientific-image-atomic-force-microscope-illustration.

40. Bhushan, B. *Springer Handbook of Nanotechnology, 3rd ed. Springer-Verlag* (2010). doi:10.1007/978-3-642-02525-9

41. Demirbaş, T. Nanotribological properties of graphene grown by chemical vapor deposition and transferred onto silicon oxide substrates. (Bilkent University, 2015).

42. Ogletree, D. F., Carpick, R. W. & Salmeron, M. Calibration of frictional forces in atomic force microscopy. *Rev. Sci. Instrum.* **67,** 3298–3306 (1996).

43. https://www.nanomagnetics-inst.com/tr/.

44. Binnig, G., Rohrer, H., Gerber, C. & Weibel, E. Surface studies by scanning tunneling microscopy. *Phys. Rev. Lett.* **49,** 57–61 (1982).

45. Binnig, G. & Quate, C. F. Atomic Force Microscope. *Phys. Rev. Lett.* **56,** 930–933 (1986).

46. Mate, C. M., McClelland, G. M., Erlandsson, R. & Chiang, S. Atomic-scale friction of a tungsten tip on a graphite surface. *Phys. Rev. Lett.* **59,** 1942–1945 (1987).

47. supplied from: https://www.spmtips.com/test-structures-TGF11-series.html.